International Journal of Biophysics 2013, 3(1A): 18-38
DOI: 10.5923/s.biophysics.201311.03

Single-molecule FRET Studies on DNA Mismatch Repair

Jeungphill Hanne[1], Jiaquan Liu[1], Jong-Bong Lee[1,2,3,*], Richard Fishel[1,4,*]

[1]Department of Molecular Virology, Immunology and Medical Genetics, The Ohio State University Medical Center, Columbus, USA
[2]Department of Physics, Pohang University of Science and Technology (POSTECH), Pohang, Korea
[3]School of Interdisciplinary Bioscience and Bioengineering, POSTECH, Pohang, Korea
[4]Physics Department, The Ohio State University, Columbus, USA

Abstract DNA mismatch repair (MMR) is the process that corrects misincorporation errors introduced by DNA polymerases during replication. MMR is also associated with other biological processes such as the suppression of recombination between partially homologous sequences (homeologous recombination) and DNA-damage signaling. Mutations of the human MMR genes are the cause of Lynch syndrome, also known as hereditary nonpolyposis colorectal cancer (LS/HNPCC). The detailed mechanism of MMR components in these biological processes remains enigmatic. MMR that is coupled to replication is an excision-resynthesis reaction. It is initiated at a distant strand scission that is 100's to 1000's of bp from the mismatch and the excision tract extends from that strand scission to just past the mismatch. MutS and MutL are unique core components of MMR that recognize a mismatch and initiate the excision reaction. Additional components include the replication clamp (β-clamp in prokaryotes and PCNA in eukaryotes), the replication clamp loader (γδδ' in prokaryotes and RFC in eukaryotes), an exonuclease (Exo1, ExoX, RecJ, ExoVII in prokaryotes and EXOI in eukaryotes), and single strand binding protein (SSB in prokaryotes and RPA in eukaryotes). Recently single molecule FRET/Fluorescent Tracking (smFRET/FT) studies have made a significant impact on understanding the MMR process. More extensive future smFRET/FT studies are expected to further detail the MMR mechanism. This review is intended to offer a guide to applying smFRET/FT studies to understand the entire MMR process, by pinpointing key questions and poorly understood phenomena. We summarize recent smFRET/FT results and address major issues in the application of the smFRET/FT system.

Keywords Total Internal Reflection Fluorescence, TIRF, ATPase, Exonuclease, Protein Interactions

1. Introduction

The concept of mismatch repair (MMR) was independently proposed in 1964 by Evelyn Witkin based on her bromo-deoxyuracil incorporation studies[1], and Robin Holliday based on his gene conversion analysis in fungi[2]. In the early 1970s the genes responsible for MMR started to be identified[3,4]. Since then the mechanism of MMR has been continuously refined[5-8]. Components of the MMR machinery have been shown to be involved in other biological phenomena such as the suppression of recombination between partially homologous DNAs (homeologous recombination)[9], and DNA-damage signaling[10-12]. Defects in core human MMR genes are the cause of Lynch syndrome also known as hereditary nonpolyposis colorectal cancer (LS/HNPCC); perhaps the most common hereditary cancer predisposition syndrome [13-18]. In this section, we briefly summarize the basic MMR process and its role in other biological processes as well as point out key unanswered questions.

1.1. Replication Coupled DNA Mismatch Repair

The basic role of MMR is to correct nucleotide misincorporation errors introduced by the DNA polymerase during DNA replication. Indeed, the MMR genes were originally identified as "mutators" (Mut) since uncorrected replication errors resulted in a 100-1000 fold increase in spontaneous mutation rates[19-21]. The core genes of MMR have been conserved through evolution (Table 1; Fig. 1)[22]. The MMR mechanism can be sequentially divided into four main steps: 1.) Recognition of a DNA mismatch, 2.) Transfer of the mismatch recognition signal to the distant strand scission site where DNA excision starts, 3.) Excision of the "newly incorporated" mismatched strand[5-8] and 4.) resynthesis of the excised DNA strand. Strand-specific excision engenders the unique steps in MMR since the resynthesis step appears to be accomplished by the normal replication polymerase machinery.

* Corresponding author:
jblee@postech.ac.kr (Jong-Bong Lee)
rfishel@osu.edu (Richard Fishel)
Published online at http://journal.sapub.org/biophysics

Table 1. DNA mismatch repair protein functions

E. coli	Yeast	Human	Overall function
MutS	Msh2-Msh3 Msh2-Msh6	hMSH2-hMSH3 hMSH2-hMSH6	Small IDLs recognition. ATP-bound sliding clamp formation Mismatch recognition. ATP-bound sliding clamp formation
MutL	Mlh1-Pms1 Mlh1-Mlh2 Mlh1-Mlh3	hMLH1-hPMS2 hMLH1-hPMS1 hMLH1-hMLH3	Coordinator of the downstream processes after mismatch recognition by MutS. GHKL ATPase. Cryptic endonuclease
MutH	-	-	Nick newly synthesized DNA strand in hemimethylated GATC sites
UvrD	-	-	Helicase. Unwind DNA to assist DNA excision by exonucleases
□ γ-δ complex	Rfc complex	RFC complex	β -clamp loading
β -clamp	Pcna	PCNA	Connect mismatch repair machinery to the replication fork
ExoI, ExoX	ExoI	hEXOI	5′ → 3′ DNA excision
RecJ, ExoVII	? [1]	? [1]	3′ → 5′ DNA excision

1. Represents unknown similar biochemical functions, or redundancy between ExoI and Mlh1-Pms1/2

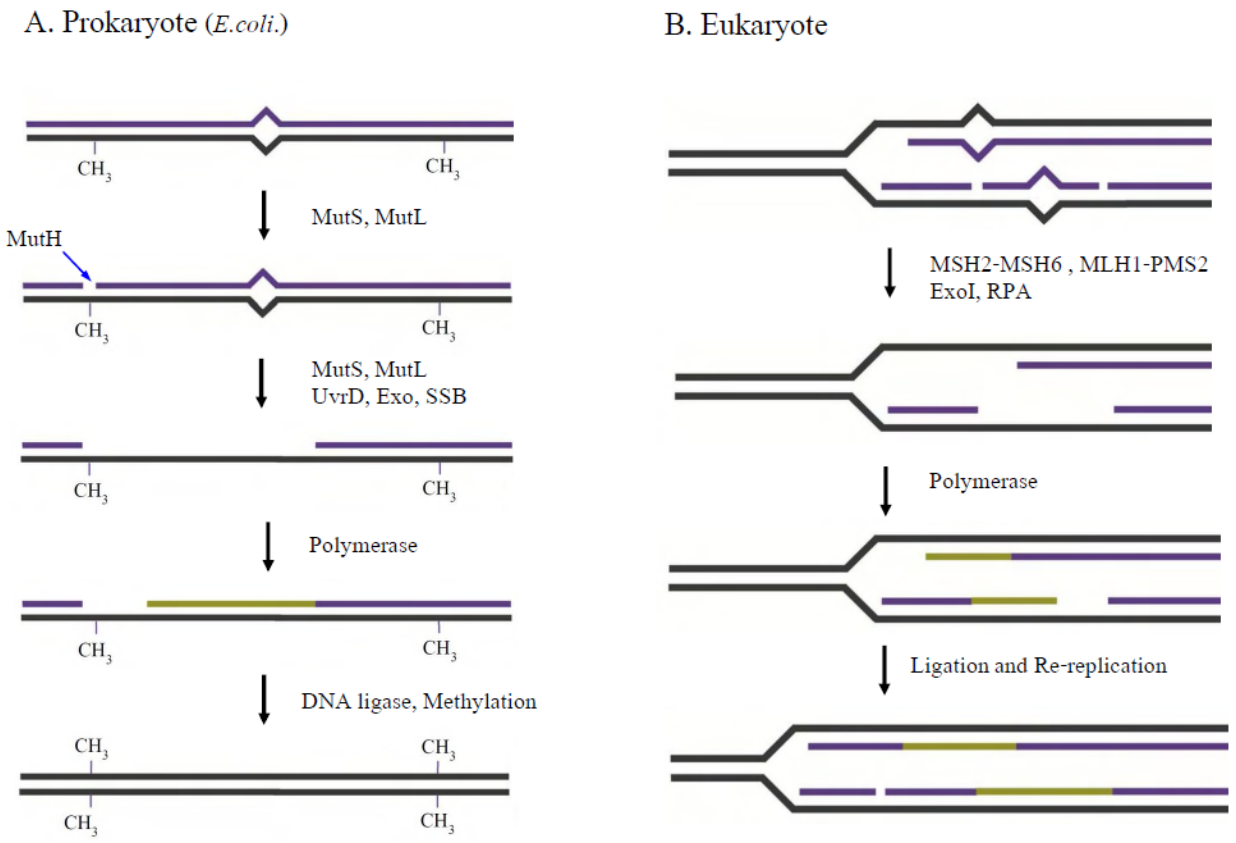

Figure 1. DNA Mismatch Repair in Prokaryote and Eukaryote Systems. A. Prokaryote MMR (gram negative enteric bacteria *E.coli*). MutS recognizes the mismatch and MutS and MutL together activate the MutH endonuclease. MutH introduces a strand scission on the unmethylated strand of a nearby hemi-methylated GATC site (-CH_3). The newly replicated strand is transiently unmethylated following replication ultimately providing strand discrimination for MMR. The strand scission serves as an entry site for the UvrD helicase and one of four exonucleases that unwind and degrade the daughter strand to just past the mismatch. *E.coli* SSB protects the template single strand DNA until the replication machinery reengages to synthesize the complementary strand. The remaining strand scission is sealed by DNA ligase, completing the MMR process. **B.** Eukaryote MMR (and prokaryote MMR other than gram negative enteric bacteria). Mismatched nucleotides are primarily recognized by MSH2-MSH6. MSH2-MSH6, MLH1-PMS2 (Pms1 in *S.cerevisae*) and EXOI degrade the mismatched strand, starting at scissions on the newly synthesized strand. The single-stranded DNA binding heterotrimer RPA protects the ssDNA gap, while the replication machinery rengages to synthesize the complementary strand. Remaining strand scissions are sealed by DNA ligase

The prokaryotic MutS protein recognizes mismatched DNA as a homodimer[23]. In eukaryotes, the MutS gene appears to have been duplicated and evolutionarily refined to form heterodimers of MutS homologs (MSH)[24-26]. The MSH2-MSH6 heterodimer primarily recognizes base-base and single nucleotide insertion mismatches, while the MSH2-MSH3 heterodimer recognizes single nucleotide insertions up to 8-12 insertion/deletion loop-type (IDL) mismatches[27-30]. The increased range of substrate specificity is presumably due to the increased complexity of the eukaryotic genome. MSH proteins are members of the AAA ATPase family[31,32]. Accumulating evidence suggests that MSH proteins normally retain at least one ADP after hydrolysis[33,34]. The ADP-bound subunit appears to control unregulated hydrolysis by MSH proteins[33]. Upon binding to a mismatch, the ADP is released allowing ATP binding by both MSH subunits. ATP binding provokes a conformational transition that results in mismatch dissociation and movement of the MSH along the adjacent DNA[30,35-39]. The ATP-bound MSH appears to attract MutL homologs (MLH/PMS; Table 1; Fig.1)[35,40] that help to transmit the mismatch binding signal to downstream MMR excision machinery. The major MLH/PMS in *Sacchromyces cerevisiae* (Sc) is ScMlh1-ScPms1 and in human hMLH1-hPMS2 (ScPms1 and hPMS2 are conserved homologs that share different numbers as a result of a historical nomenclature accident)[5-8].

The MMR excision tract in both prokaryotes and eukaryotes have two important features: 1.) It is strand specific; occurring uniquely on the newly replicated strand thereby decreasing the potential for mutations, and 2.) Excision may occur 5'→3' or 3'→5' towards the mismatch (Bidirectionality). In the gram-negative enteric bacteria *E.coli* the MutS-MutL complex activates the MutH endonuclease. GATC sequences are normally symmetrically methylated throughout the *E.coli* genome by the *D*NA *a*denine *m*ethylase (Dam)[41]. MutH introduces a strand scission on the unmethylated strand of a nearby GATC sequence that is transiently unmethylated on the newly replicated strand (Fig. 1A)[42]. This strand scission serves as an entry site for the UvrD helicase and one of four exonucleases (Fig. 1A; 3'→5' exonucleases RecJ and ExoVII; 5'→3' exonucleases ExoI and ExoX)[43] that unwind and degrade the daughter strand to just past the mismatch[44-46]. *E.coli* SSB protects the template single strand DNA until the replication machinery engages again to resynthesize the complementary strand. The remaining strand scission is sealed by DNA ligase, completing the MMR process[46]. The mechanism for introducing strand specificity (strand specific scission) and bidirectionality in all other bacteria except gram-negative enteric bacteria including eukaryotes is largely unknown.

One of the major questions associated with the MMR mechanism is how the MSH mismatch-recognition signal is transferred to the site where the exonuclease-dependent excision is initiated; typically 100's to 1000's of nucleotides distant from the mismatch. Three different conceptual models have been proposed (Fig. 2)[47]: 1.) Static Transactivation[48], 2.) Hydrolysis-Dependent Translocation[49,50], and 3.) Molecular Switch Sliding Clamp[35,37, 38,51]. In the Static Transactivation model, often referred as "trans-activation or stationary model", the MSH or a complex of MSH and MLH/PMS capture a 3D looping of DNA to authorize the distant site where an exonuclease can start to degrade the newly replicated strand. However, this model has been largely disproven since artificial blocks on the presumably unimportant intervening looped DNA block MMR[52]. The other two models, described as "cis-activations or moving models", propose movement of the MSH protein or the MSH-MLH/PMS complex along the DNA. ATP binding and hydrolysis by the MSH and MLH/PMS are proposed to elicit movement of a single complex to the target site in the Hydrolysis-Dependent Translocation model (Fig. 2)[49,50]. In contrast, the Molecular Switch Sliding Clamp model suggests that multiple MSH-MLH/PMS complexes are loaded and that movement to the target site is driven by thermal diffusion (Fig. 2)[35,37,38,51]. The multiple sliding clamps provoke short DNA excision tracts starting at the DNA scission in a dynamic and redundant process until the mismatch loading site is eliminated. It is termed the Molecular Switch Sliding Clamp model since the mismatch provokes exchange of ADP→ATP exchange similar to the activation of G-protein switches[53], and ATP binding induces a conformational transition that ultimately results the formation of a sliding clamp where movement occurs without ATP hydrolysis [35,38].

As suggested above, outside of gram-negative enteric bacteria and including eukaryotic systems, the overall MMR picture is similar. But there is no homolog for MutH and no counterpart has been found for the 3'-5' exonucleases RecJ and ExoVII. These observations suggest important differences in the details of MMR in these organisms. Moreover, without a MutH the mechanism of strand discrimination requires elucidation. Several pieces of evidence suggest that a preexisting nick in the daughter strand provides the strand discrimination that is recognized by the MMR machinery. Theoretically, transient strand scissions exist in the leading (3'-replication end) and the lagging (5'- and 3'-end of the Okazaki fragment) daughter strand during replication and prior to ligation (Fig. 1B).

Evidence suggests that the complete MMR reaction in eukaryotes can occur from a 5' strand scission without an MLH/PMS[54]. In contrast, MMR from a 3' strand scission requires MLH/PMS[55]. A further dilemma is that the only exonuclease found to be associated with eukaryotic MMR is ExoI; a 5'→3' exonuclease[56-58]. These observations raise the question of how a 3'→5' MMR excision tract is formed? A few years ago the hPMS2 was found to harbor a cryptic endonuclease[59]. Moreover, mutation of the conserved endonuclease domain in the MutL of the gram-positive bacteria *Bacillus subtilis* (BsMutL) or the ScPms1 displayed a mutator phenotype consistent with an MMR defect[60-62]. Finally, conformational transitions within the BsMutL

endonuclease appear to be regulated by a separate Zn-binding domain[61]. It has been postulated that the MLH/PMS endonuclease creates a 5'-scission on the 3'-side of the mismatch that is then a substrate for EXOI[59]. Another possibility is that the MLH/PMS endonuclease is redundant with EXOI, which would explain the relatively low mutator activity of *exoI* mutations in *S.cerevisae*[63,64]. Details such as the mechanism of daughter strand targeting, fragment size, and protein-DNA interaction are unknown.

In addition to these DNA transaction questions there are numerous protein-protein interactions that result from multifaceted temporal interactions during MMR. Time resolved complexes include bacterial MutS-MutL, MutS-MutL-MutH, and MutL-β-clamp as well as human hMSH2-hMSH6-hMLH1-hPMS2, (hMSH2)hMSH6-PCNA, hMSH2(hMSH6)-hEXOI, (hMSH2)hMSH3-hEXOI, and hMLH1(hPMS2)-hEXO1 that are known to date (Table 2A; genes in parenthesis are heterodimeric partners that are presumed to tag along during protein-protein interactions).

1.2. Suppression of Homologous Recombination by DNA Mismatch Repair

MMR suppresses recombination between partially homologous sequences (homeologous recombination) [9,65,66]. The mechanism is unknown. Early studies suggested that MMR components inhibited the strand exchange reaction (recombinase) catalyzed by the central recombination-initiation protein RecA[67]. However, since both MutS and MutL may individually bind single-stranded DNA (ssDNA), it remains formally possible that the observed inhibition of RecA recombinase was a result of competition for the homologous donor ssDNA rather than discrimination between partial homology with the acceptor double-stranded DNA (dsDNA). Other possible mechanisms would include: 1.) recognition of mismatches in the D-loop recombination initiation intermediate that provokes MMR excision and ultimately release of the invading donor ssDNA, or 2.) MMR-dependent incision of the D-loop that would release the superhelicity required to stabilize the homologous donor ssDNA. It is also possible that aspects of both these models are operable.

1.3. Involvement of DNA Mismatch Repair in DNA-damage Signaling

MMR deficient cells are at least 100-fold more tolerant to the exposure of various toxic agents that damage DNA. It has been suggested that MMR proteins act as damage sensors that initiate an apoptotic response following overwhelming or unrepairable DNA damage[10,68]. Remarkably, MMR components appear to directly interact with the ATR/ATRIP signaling components following DNA damage[69]. The damage signaling process appears far more complex than MMR and the suppression of homeologous recombination since it involves chromatin, chromatin structure and long-range diffusible signaling processes.

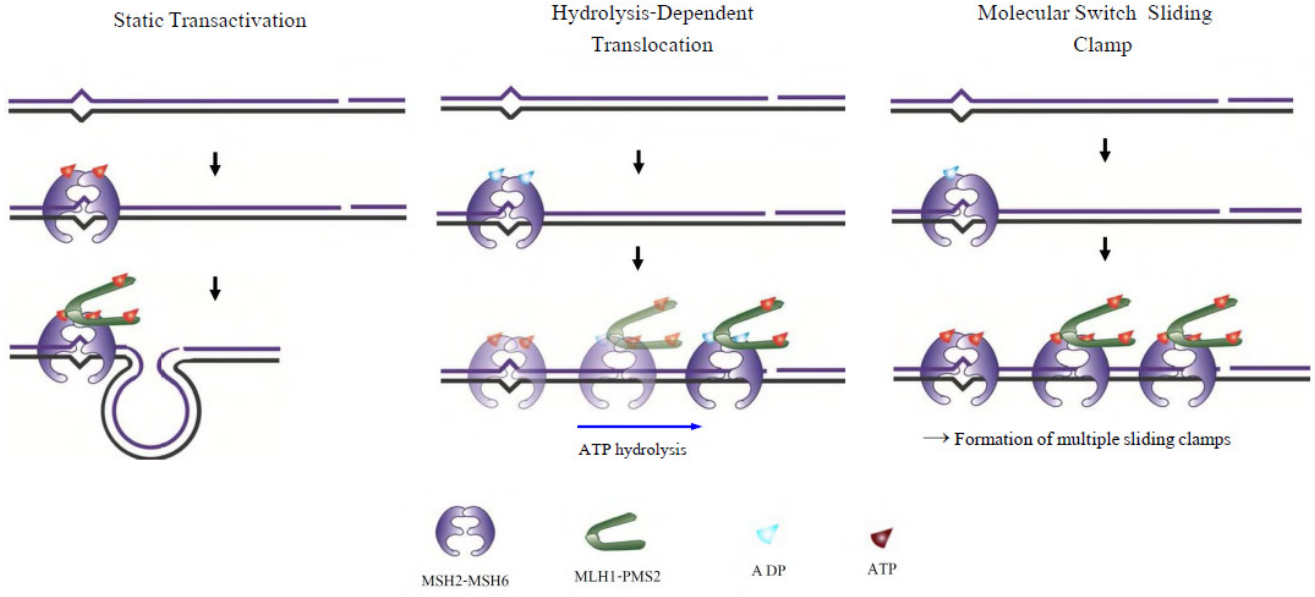

Figure 2. Models for the Mismatch Recognition and Downstream Signal Transfer. Left) Static Transactivation. The MSH or a complex of MSH and MLH/PMS capture a random loop of DNA to authorize the distant site where helicase/exonuclease may start degradation of the newly replicated strand. **(Center)** Hydrolysis-Dependent Translocation. ATP binding and hydrolysis by the MSH and MLH/PMS elicit movement to the distant target site where helicase/exonuclease may start degradation of the newly replicated strand. **(Right)** Molecular Switch Sliding Clamp. The mismatch-dependent ATP-binding provokes a conformational transition of MSH into a stable sliding clamp on the DNA that recruita MLH/PMS. Movement of MSH-MLH/PMS complex is driven by thermal diffusion that ultimately reaches to the distant excision-initiation site

Table 2. Minimal MMR process and multiple protein-protein interactions

(a) Minimal complete MMR process

	2~3 components	**3~4 components**	**3~4 components**	**4, or more components**
MutL indep. MMR	MutS + ExoI	MutS + ExoI + RPA	MutS + ExoI + PCNA	MutS + ExoI + PCNA+ RPA
MutL dep. MMR	MutS + ExoI + MutL	MutS + ExoI + RPA + MutL	MutS + ExoI + PCNA + MutL	MutS + ExoI + PCNA+ RPA + MutL
MutH dep. MMR	MutS + MutL + ExoI,(or ExoX) or, MutS + MutL + ExoVII,(or RecJ)	MutS + MutL + ExoI,(or ExoX) + SSB or, MutS + MutL + ExoVII,(or RecJ) + SSB	MutS + MutL + ExoI,(or ExoX) +β clamp or, MutS + MutL + ExoVII,(or RecJ) + β clamp	MutS + MutL + ExoI, (or ExoX) + ExoVII, (or RecJ) β+ clamp
Features	Mismatch Recognition/Removal	+ protection	+ facilitation ?	Close to *in vivo case*

(b) Multiple protein-protein interactions involved in MMR

Multiple protein-protein interactions	**Features**
MutS + MutL	• Early data obtained by single molecule studies • Relatively elaborate explanation from previous bulk studies
MutS+ ExoI	-
MutL+ ExoI	-
MutS +PCNA	• Relatively elaborate explanation from previous bulk studies
MSH2-MSH3 + PCNA	-
MutL+ PCNA	-
ExoI+ PCNA	-
MutH + MutL	-

1.4. Lynch Syndrome

The majority of Lynch syndrome or hereditary non-polyposis colorectal cancer (LS/HPNCC) is caused by defects in the human MMR genes[70]. The majority of mutations have been found in the hMSH2 and hMLH1 genes, with approximately 10% of mutations occurring in hMSH6 and hPMS2[70]. MMR defects are thought to drive cancer by elevating mutation rates (Mutator Hypothesis;[71]. However, LS/HNPCC patients are heterozygous for MMR defects while the disease penetrance suggests that affected family members have a greater than 90% chance of developing cancer in their lifetime[70]. This observation suggest that mutation of the remaining normal MMR gene copy may have a "selective advantage", which should not be the case for simple MMR defects that only increase the rate of spontaneous mutations *after* the normal copy is mutated. The explanation for this conundrum appears to be the role of MMR in damage signaling. For example, when confronted with excessive DNA damage, cells containing even one copy of the MMR genes will signal apoptosis normally[72]. In contrast, a cell with an MMR defect will tolerate the DNA damage, survive, and then in subsequent cell divisions accumulate mutations from which the numerous genetic alterations that are found in cancer cells can arise[10,68].

1.5. The Development of FRET in MMR Studies

Until recently, there were no definitive experimental methodologies capable of authenticating the interactions and mechanisms associated with MMR. However, single molecule FRET/Fluorescent Tracking studies (smFRET/FT) have begun to provide substantial quantitative and visual evidence for the Molecular Switch Sliding Clamp MMR model[36,39,73]. These initial results suggest that single molecule analysis has the capability of visualizing and characterizing the entire MMR mechanism. Incorporating

FRET into single molecule applications provides extremely accurate nanometer (nm) distance measures between individual protein particles containing either a donor or acceptor fluorophore[74]. The advantage to smFRET/FT includes the ability to image molecules in real-time, the ability to observe intermediate populations, fast acquisition times (usually in the low msec range), and single particle tracking with nm resolution. Latter sections will describe in more detail how the molecular mechanisms associated with the MMR reaction has been advanced using smFRET/FT analysis and what further studies are required.

2. Single Molecule Studies of MMR

2.1. Muts Homologs

The functional analysis of the MutS homologs has taken center stage in both bulk and single molecule studies because of its central role in MMR initiation. This section will focus on the historical development of single molecule FRET analysis of MutS homologs with particular focus on results that could not be obtained by any other methodology.

Mismatch recognition and its signal transfer – In 2007, the era of MMR single molecule analysis opened when the yeast MutS homologs, ScMsh2-ScMsh6, were shown to diffuse on duplex DNA[75]. These initial observations used a unique smFT system that attached "curtains" of λ DNA to an engineered groove in a flow cell. This allowed the video capture and analysis of hundreds of DNA molecules that were bound across the horizontal groove and were stretched by laminar flow. The ScMsh2 protein within the ScMsh2-ScMsh6 heterodimer contained a His_6-tag that could be bound by a anti-His antibody that was labeled with a Quantum Dot (qDot). Movement of the ScMsh2-ScMsh6-antiHis-qDot was tracked on individual λ DNA molecules by prism-based Total Internal Reflection Fluorescent (TIRF) microscopy where the critical angle of an excitation laser is controlled by a prism above the flow cell. An optical filtered charge coupled devise (CCD) camera captured the qDot emission fluorescence through the objective lens of the microscope.

These studies visualized diffusion of ScMsh2-ScMsh6 on duplex DNA in a neutral buffer with 50 mM salt. The authors concluded that ScMsh2-ScMsh6 likely diffused on duplex DNA with rotation by comparing the measured diffusion coefficient with theoretical 1D-diffusion with rotation or purely translational 1D-diffusion constants. The result seemed to imply that MutS homologs search for mismatches on duplex DNA by tracking the DNA helix. Remarkably, these studies also observed several ScMsh2-ScMsh6 proteins with very long lifetimes. These observations were used to support a Static Transactivation model. Later studies from the same group[73] as well as others[36,39] have disputed these long-lived species; suggesting they were unusual and/or rare protein events that arose from either the low ionic conditions, the non-equilibrium flow-system or the qDot labeling technique. It is also important to note that the combination of qDot-labeled anti-His antibody required for fluorescent visualization is larger than the ScMsh2-ScMsh6 heterodimeric protein, raising the question of whether the visualization method may have unduly influenced the diffusion analysis from its beginnings. The authors argue against this possibility in supplemental calculations[75]. However, such long-lived MSH species are rarely observed in the absence of flow systems and qDot labeling[36,39]. The ability to observe and trap rare events can be both valuable and misleading with single molecule analysis.

Although these authors visualize for the first time how an MSH interacted with duplex DNA, many more questions remained unanswered such as: its behavior in physiological salt (100-150 mM), the lifetime of MSH's on DNA, the interaction(s) with mismatched DNA, ATP and ADP dependences, among others.

To address these specific questions, a unique smFRET system was designed (Fig. 3)[39]. These investigators used *Thermus aquaticus* MutS (TaqMutS), which containes only one Cys residue (C42) that could be labeled with a single Cy3 fluorophore using maleimide chemistry (Fig. 3A). Unfortunately the protein was completely inactivated by the C42-Cy3 label since it was located in a domain that is used to interrogate mismatched DNA (Fig. 4)[31,32]. To solve this problem, C42 was mutated to an Ala (C42A) that had no effect on TaqMutS function. Then a Thr residue (T469) on the outside surface of the TaqMutS protein was changed to a Cys (T469C) and labeled with Cy3 that had no effect on TaqMutS function (Fig. 3A). Using FRET between Cy3 on TaqMutS and Cy5 on the DNA, the lifetime of TaqMutS on duplex DNA and DNA containing a mismatch was examined in near physiological conditions (100mM salt; Fig. 3). Remarkably, the lifetime of TaqMutS on duplex DNA was 10-fold shorter when the surface-bound DNA contained an open-end compared to when it was blocked with an anti-digoxigenin antibody (0.31s compared to 3.7s; Table 3; Fig. 3B and 3C; TaqMutS lifetime $\tau_{duplex \cdot off}$ for unblocked DNA may be calculated as the inverse of the $k_{duplex \cdot off}$ = 3.2 s^{-1}). This result strongly suggested that the MutS protein formed an incipient clamp on duplex DNA that was retained when both ends are blocked (biotin-streptavidin on the surface and dig-antidig). While biochemical and structural analysis suggested that MSH proteins formed a clamp when bound with ATP[38] and when bound to a mismatch (Fig. 4)[31,32], this was the first direct evidence that MSH proteins formed a clamp while searching for a mismatch on duplex DNA. It was the short time resolution provided by this smFRET system (30ms) that allowed the lifetime measures of TaqMutS on blocked and unblocked duplex DNA.

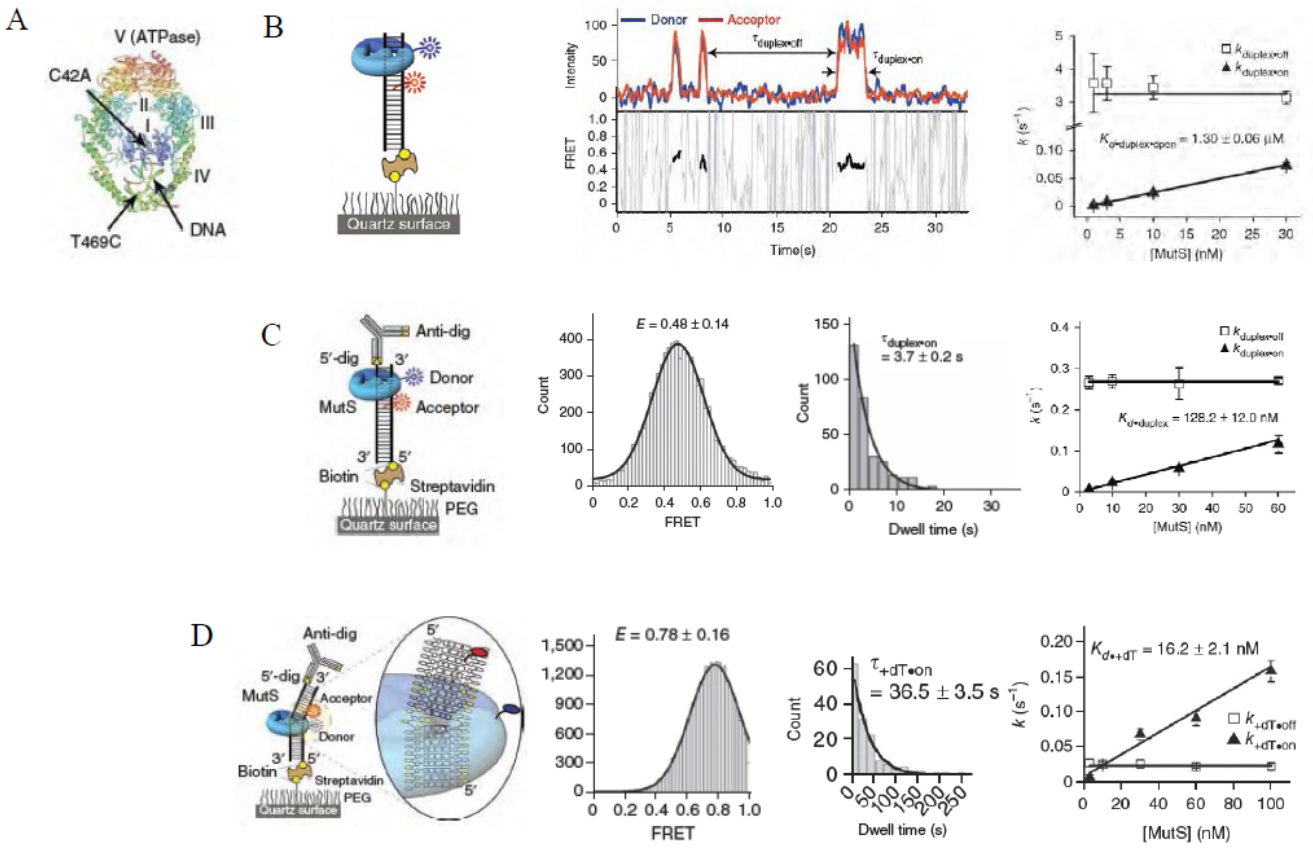

Figure 3. smFRET Analysis of TaqMutS Association with Duplex DNA. A. Structure of TaqMutS bound to a mismatch showing peptide domains I–V (PDB 1EWQ)42. Donor Cy3 was conjugated to Cys469 of TaqMutS(C42A,T469C). **B.** (left) Schematic representation of smFRET assay with the duplex DNA containing an open end. Cy5-labeled duplex DNA molecules (74 bp) were immobilized on a quartz surface via a biotin-streptavidin linker. (center) representative kinetic scan showing TaqMutS binding lifetime ($\tau_{duplex\cdot on}$) and dissociation lifetime ($\tau_{duplex\cdot off}$). (right) Determination of $K_{d\cdot duplex\cdot open}$ from $k_{duplex\cdot off}$ ($1/\tau_{duplex\cdot off}$) that was independent of TaqMutS concentration and the slope of $k_{duplex\cdot on}$ ($1/\tau_{duplex\cdot on}$) versus TaqMutS protein concentration. **C.** (left) Schematic representation of smFRET assay with the duplex DNA containing blocked ends. The "free" end is blocked with anti-digoxigenin (anti-dig) and while the remaining end is bound to the surface via a biotin-streptavidin linkage. (center) The FRET efficiency and distributions of binding lifetime for 10 nM MutS in 100 mM KCl. A single exponential with mean ± s.e.m. fit the distribution. (right) The $K_{d\cdot duplex\cdot blocked}$ determined as in B(right) above. **D.** (left) Schematic representation of smFRET assay with the mismatched DNA containing blocked ends. (center) The FRET efficiency and distributions of binding lifetime for 10 nM MutS in 100 mM KCl. A single exponential with mean ± s.e.m. fit the distribution. (right) The $K_{d\cdot mismatch}$ determined as in B(right) above. **(taken from Jeong *et al.*, 2011)**

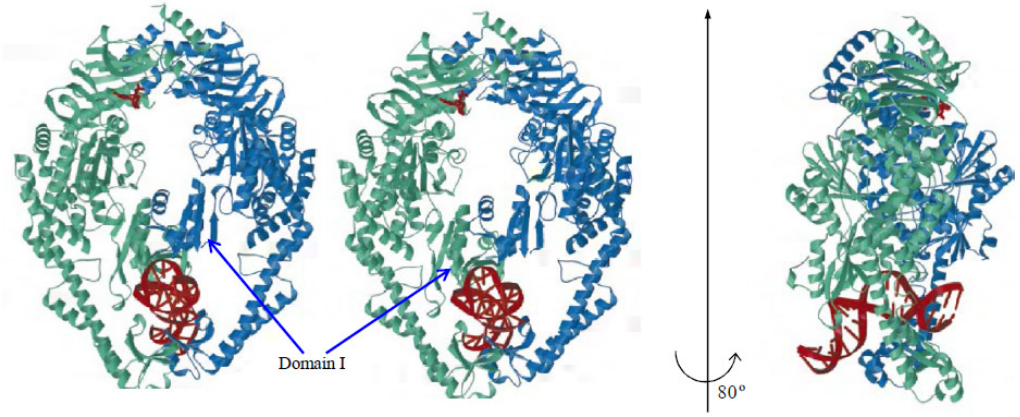

Figure 4. The structure of MutS binding to mismatched DNA. DNA and ADP are colored red, the mismatch-binding monomer light green, and the second monomer blue **A.** Front view. Mismatch interrogation Domain I is identified with arrows. **B.** Side view. Rotated from (A) by 80°

Table 3. Comparison of smFRET/FT data on the MutS homolog

	Taq MutS (~170kDa : Homo-dimer)			**Yeast Msh2-Msh6** (~260kDa : Hetero-dimer)
Research groups	Jeong C *et al* [1] Cho WK *et al* [2]	Sass LE *et al* [3]	Qiu R *et al* [4]	Gorman J *et al* [5]
Searching time[sec] @150mM NaCl	~ 1	-	-	~ 20
Lifetime at the mismatch[sec]	~ 35	~13	~ 2.25	~ 580
Transient lifetime on the mismatch in the presence of ATP[sec]	~ 3	-	-	-
Lifetime of the sliding clamp[sec]	~ 680	-	-	Over 198
Methods	smFRET/FT [6]	smFRET [7]	smFRET [8]	smFT

1. Jeong, C., Cho, W.K., Song, K.M., Cook, C., Yoon, T.Y., Ban, C., Fishel, R., and Lee, J.B. (2011). MutS switches between two fundamentally distinct clamps during mismatch repair. Nat Struct Mol Biol 18, 379-385.
2. Cho, W.K., Jeong, C., Kim, D., Chang, M., Song, K.M., Hanne, J., Ban, C., Fishel, R., and Lee, J.B. (2012). ATP alters the diffusion mechanics of MutS on mismatched DNA. Structure 20, 1264-1274.
3. Sass, L.E., Lanyi, C., Weninger, K., and Erie, D.A. (2011). Single-molecule FRET TACKLE reveals highly dynamic mismatched DNA- MutS complexes. Biochemistry 49, 3174-3190.
4. Qiu, R., DeRocco, V.C., Harris, C., Sharma, A., Hingorani, M.M., Erie, D.A., and Weninger, K.R. (2012). Large conformational changes in MutS during DNA scanning, mismatch recognition and repair signalling. Embo J 31, 2528-2540.
5. Gorman, J., Wang, F., Redding, S., Plys, A.J., Fazio, T., Wind, S., Alani, E.E., and Greene, E.C. (2012). Single-molecule imaging reveals target-search mechanisms during DNA mismatch repair. Proc Natl Acad Sci U S A 109, E3074-3083.
6. FRET between Taq MutS and the mismatch on DNA
7. FRET is occurred from the bending of DNA caused by the mismatch binding of Taq MutS
8. FRET between Taq MutS and the mismatch on DNA

As might be expected, the lifetime of TaqMutS on the DNA containing a mismatch was 10-times longer than on duplex DNA without a mismatch (36.5s; Table 3; Fig. 3D). Moreover, one could observe two distinct FRET efficiencies with these two different DNA substrates. Searching TaqMutS on the 74 bp duplex when both ends were blocked displayed an intermediate FRET (E = 0.48; Fig. 3C). Theoretical calculations suggested a protein the size of TaqMutS could transit the 74 bp duplex DNA substrate used in these studies in ~2ms. These results suggested that the intermediate FRET resulted from time averaged locations spanning the entire duplex DNA length. When TaqMutS was bound to the mismatch it exhibited a high FRET state that correlated with theoretical distance calculations between the Cy3-protein donor fluorophore from the Cy5-labeled DNA acceptor fluorophor located 9 nucleotides away from the mismatch (E = 0.78; Fig. 3D).

When ATP was added to the system (the physiological condition), one could identify three temporal FRET transitions that also corresponded with unique lifetimes. These were best resolved using a slightly longer DNA containing a mismatch (100 bp; Fig. 5A). The first transition displayed an intermediate FRET (E = 0.35) and a lifetime of ~1s, while the second transition displayed a high FRET (E = 0.80) and a lifetime of ~3s (Table 3; Fig. 5B). These intermediates correspond to the mismatch searching TaqMutS and mismatch-bound TaqMutS as detailed above. The transition to the third temporal intermediate displayed an intermediate FRET (E = 0.35) similar to the mismatch searching TaqMutS, but the lifetime extended beyond the photobleaching of the Cy3-Cy5 dyes. This problem led the authors to develop a time-lapse smFRET system where they then showed that the lifetime extended to nearly 10 min (598s; Fig. 5C). Together, these results were the first to demonstrate the time-dependent transition of a MutS homolog from searching, to mismatch binding, to ATP-bound sliding clamp and confirmed the power of smFRET. The intermediate FRET suggested free-diffusion of the trapped ATP-bound TaqMutS. Moreover, substitution of the poorly hydrolyzably analogue of ATP, ATPγS, for ATP resulted in virtually identical lifetimes of the TaqMutS sliding clamp (Fig.5C, right panels). These observations were consistent with hydrolysis independent movement: a defining concept for the Molecular Switch Sliding Clamp MMR model.

Like the studies before them (see above), these authors introduced some theoretical modeling to conclude that TaqMutS rotated with the DNA helix during the mismatch searching process. Not satisfied with this result, the group went on to design smFRET/FT and single molecule polarization TIRF (smPolarizationTIRF) systems to specifically examine the diffusion and rotational dynamics of the searching, mismatch bound and ATP-bound sliding clamp forms of TaqMutS[36]. The smFRET/FT was the first to place a large single DNA molecule (15 Kb) containing a single mismatch and a Cy5 nearby the mismatch within a TIRF field (Fig. 6A and 6B). One could then track Cy3-TaqMutS on the DNA when it slid on to the mismatch (high Cy3 or green emission; Fig. 6C), when it bound to the mismatch (reduced Cy3 or green emission with corresponding increased Cy5 or red emission indicating FRET; Fig. 6C and 6D), and finally ATP-bound sliding clamp formation (reduced Cy5 or red emission indicating FRET near the mismatch to green or Cy3 emission) as the

Cy3-TaqMutS slides away from the Cy5 near the mismatch. In these studies smFRET was used to clearly identify molecules that were loaded onto the DNA at the mismatch, while the smFT allowed the quantitative analysis of the dwell-time as well as calculation of the diffusion coefficient and drift rate (Fig. 6E, 6F, 6G). Importantly, the loading of multiple ATP-bound MSH sliding clamps as predicted by the Molecular Switch Sliding Clamp model was visually confirmed[36]. Yet perhaps the most important observation in these studies was the demonstration that the diffusion coefficient of searching TaqMutS was independent of salt concentration, while the diffusion coefficient of the ATP-bound TaqMutS sliding clamp increased with salt. Theoretical analysis by von Hipple and colleagues[76] suggested that the salt concentration independent diffusion of searching TaqMutS indicated protein diffusion while in *continuous* contact with the DNA. In contrast, the increasing diffusion coefficient of TaqMutS when in the ATP-bound sliding clamp form indicated diffusion while in *discontinuous* contact with the DNA. It should be noted that the smFT system used by these authors employed hydrodynamic flow to "stretch" the DNA along the surface within the TIRF field. While several supplementary studies demonstrated than the flow system had no observable effect on the diffusion characteristics within the investigational parameters, a comprehensive theoretical and experimental analysis has not been performed.

Direct examination of rotational diffusion dynamics - To answer the question of whether the TaqMutS molecules were rotating while diffusing along the DNA, smPolarizationTIRF was developed[36]. In this system, rotationally polarized light was used to illuminate the TIRF field and filters distinguished the horizontal and vertical components (Fig. 7A). Such a system is only viable if the fluorophore bound to the TaqMutS does not depolarize faster than the acquisition time. To test this issue, the authors bound the Cy3-TaqMuts to the surface and determined the polarization distribution. The results demonstrated that the surface-bound TaqMutS exhibited a wide range of polarization distribution presumably depended on its random surface orientation, suggesting that the Cy3 fluorophore was constrained (Fig. 7B). Moreover, TaqMutS that was bound to a mismatch also displayed a broad polarization distribution that indicated it was tightly bound to the mismatch on randomly oriented, but relatively fixed, DNA[36].

The authors then realized that a protein rotating along a short oligonucleotide DNA backbone would display no net polarization until the DNA length approached the protein footprint on the DNA. When the DNA length approached the footprint, the protein would be constrained from time-averaged rotational diffusion and would have a broad polarization distribution; analogous to being bound on the surface (or a mismatch). Taking advantage of this concept, they measured the polarization distribution of searching TaqMutS and ATP-bound TaqMutS sliding clamps at different DNA lengths (Fig. 7C-G). Remarkably, searching MutS displayed a broad polarization distribution as the DNA length approached the protein footprint (Fig. 7C, 7E,and 7G). Combined with the diffusion dynamics, these studies conclusively demonstrated that TaqMutS searches for a mismatch by rotational diffusion while in *continuous* contact with the DNA backbone. In contrast, the ATP-bound TaqMutS sliding clamps displayed no net polarization regardless of DNA length (Fig. 7D, 7F, and 7G). Combined with the diffusion dynamics, these studies conclusively demonstrated that ATP-bound TaqMutS sliding clamps rotate freely around the DNA while in *discontinuous* contact with the DNA backbone. The use of these unique smFRET/FT and smPolarizationTIRF appeared to fully define for the first time the diffusion mechanics of MSH proteins during the mismatch search, mismatch binding and sliding clamp formation.

Virtually all of these observations were later confirmed for the ScMsh2-ScMsh6 protein using the smFT DNA curtain system[73]. A compilation of lifetime measures is shown in Table 3. We note several differences that could easily be attributed to the larger size of the ScMsh2-ScMsh6 that is bound with antibody-labeled qDots (see above), as well as other non-physiological issues such as the fact that TaqMutS activities are by nature examined at ambient temperatures (23-25^{o}C) rather than the 95-100^{o}C temperatures where *Thermus aquatics* exists in nature. One intriguing non-finding by the *Gorman et al.,* group was the transition lifetime of ScMsh2-Msh6 on the mismatch in the presence of ATP. This group generally appears to set up the system by binding ScMsh2-Msh6 on the mismatch and then pulsing it with ATP. These are not exactly the physiological condition where ATP is continuously present. Moreover, the enormously long lifetime of ScMsh2-Msh6 on the mismatch in the absence of ATP may be due to the fact that the λ DNAs contained 3 adjacent mismatches instead of a single mismatch as in the *Jeong et al.,*[39] and *Cho et al.,*[36] studies.

Caveats in single molecule FRET analysis of MutS homologs - The attraction of single molecule analysis can be overwhelming since it provides an opportunity to visualize biological reactions in real time. However, there are many pitfalls to the use of these techniques. *Sass et al.,* used smFRET combined with *t*ransition *a*nalysis *c*ombined with *k*inetic *l*ifetime *e*xamination (TACKLE)[77]. The system employed TAMRA donor and Cy5 acceptor fluorophores that were 8bp and 10bp on either side of the mismatch at the end of a 50-mer[77]. The idea was that when the DNA was unbound its native persistence length would essentially maintain the fluorophores at their maximum distance. However, when TaqMutS bound the mismatch the DNA would be bent (see Fig. 4) and increased FRET between the fluorophores would occur[77].

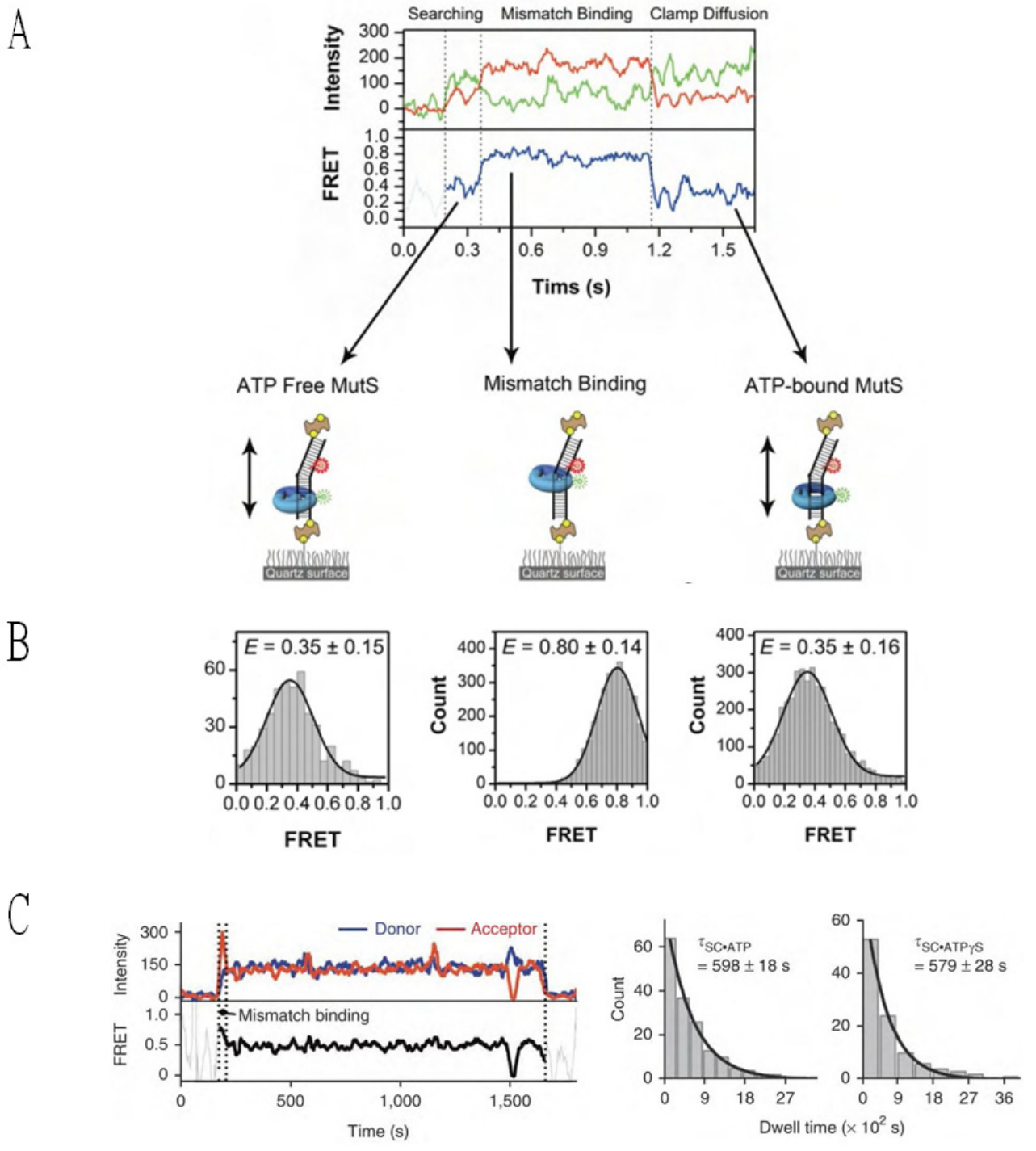

Figure 5. Kinetic Analysis of TaqMutS Association with Mismatched DNA in the Presence of ATP. A. Representation scan of TaqMutS association with 100 bp DNA containing a +dT mismatch during mismatch searching (ATP free MutS), binding (Mismatch Binding), and ATP processing (ATP-bound MutS). **B.** Histogram of FRET efficiency during the MutS search (0.35 ± 0.15), binding (0.80 ± 0.14), and ATP–induced clamp diffusion (0.35 ± 0.15) on the 100 bp DNA containing a +dT mismatch, respectively. The error bars are obtained from the s.d. **C.** (left) Representative time-lapse trace of ATP-bound Taq MutS on the +dT mismatched DNA substrate. (right) Dwell time of the sliding clamp FRET state of MutS in the presence of ATP and ATPγS determined from a single exponential of a population histogram of +dT molecules. **(taken from Jeong *et al.*, 2011)**

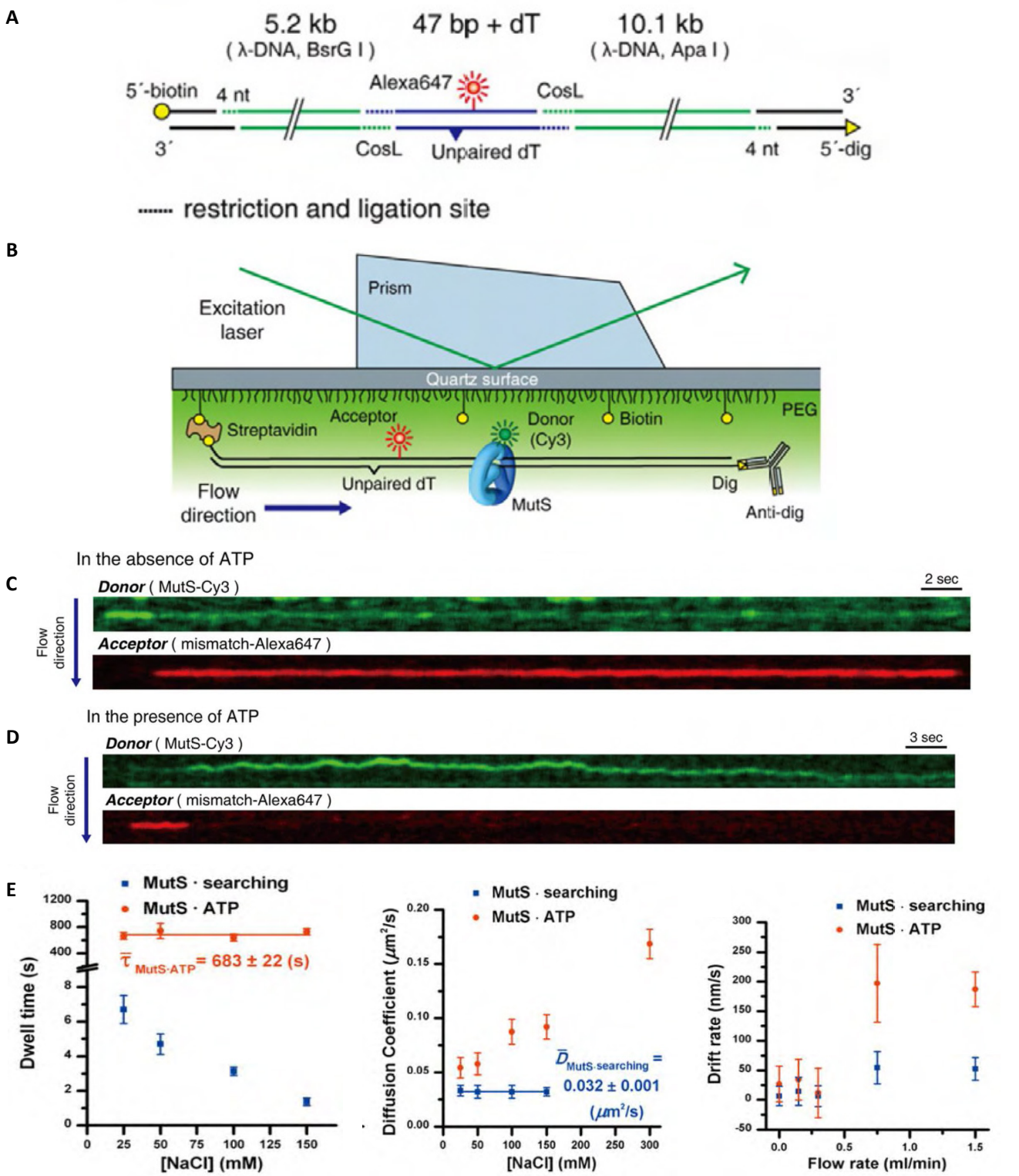

Figure 6. Single-Molecule Tracking of MutS on DNA. A. Illustration of the 15.3 kb DNA used for smFlow-FRET. **B.** A schematic representation of smFlow-FRET using prism-type total internal reflection fluorescence (TIRF) microscopy. **C.** A representative kymograph that shows searching MutS (strong green signal), followed by mismatch binding (reduced green signal; increased red FRET) in the absence of ATP. **D.** A representative kymograph of Cy3-MutS mismatch interaction(s) in the presence of ATP (200 mM). FRET emission by Alexa647 (red) indicates mismatch binding, followed by the formation of an ATP-bound MutS sliding clamp. **E.** The Distinct Diffusion Mechanism of Searching MutS and ATP-Bound MutS. **(left)** The dwell times of the Cy3-MutS on a 100 bp duplex DNA (blue) and ATP-bound MutS on a 100 bp DNA containing an unpaired dT mismatch (red; τ, $\tau_{\text{MutS•ATP}} = 683 \pm 22$ s, mean ± s.e.) as a function of ionic strength. For the ATP-bound Cy3-MutS time-lapse smFRET was exploited (see Jeong et al., 2011). **(center)** The diffusion coefficients of searching Cy3-MutS (blue; , $\tau_{\text{MutS•searching}} = 0.032 \pm 0.001$ μm^{2}s^{-1}, mean ± s.e.) and ATP-bound Cy3-MutS (red) on the 15.3 kb DNA containing a mismatch at various salt concentrations (25, 50, 100, and 150 mM NaCl). **(right)** The drift rate of protein trajectories versus flow rate. All error bars indicate s.e. **(taken from Cho *et al.*, 2012)**

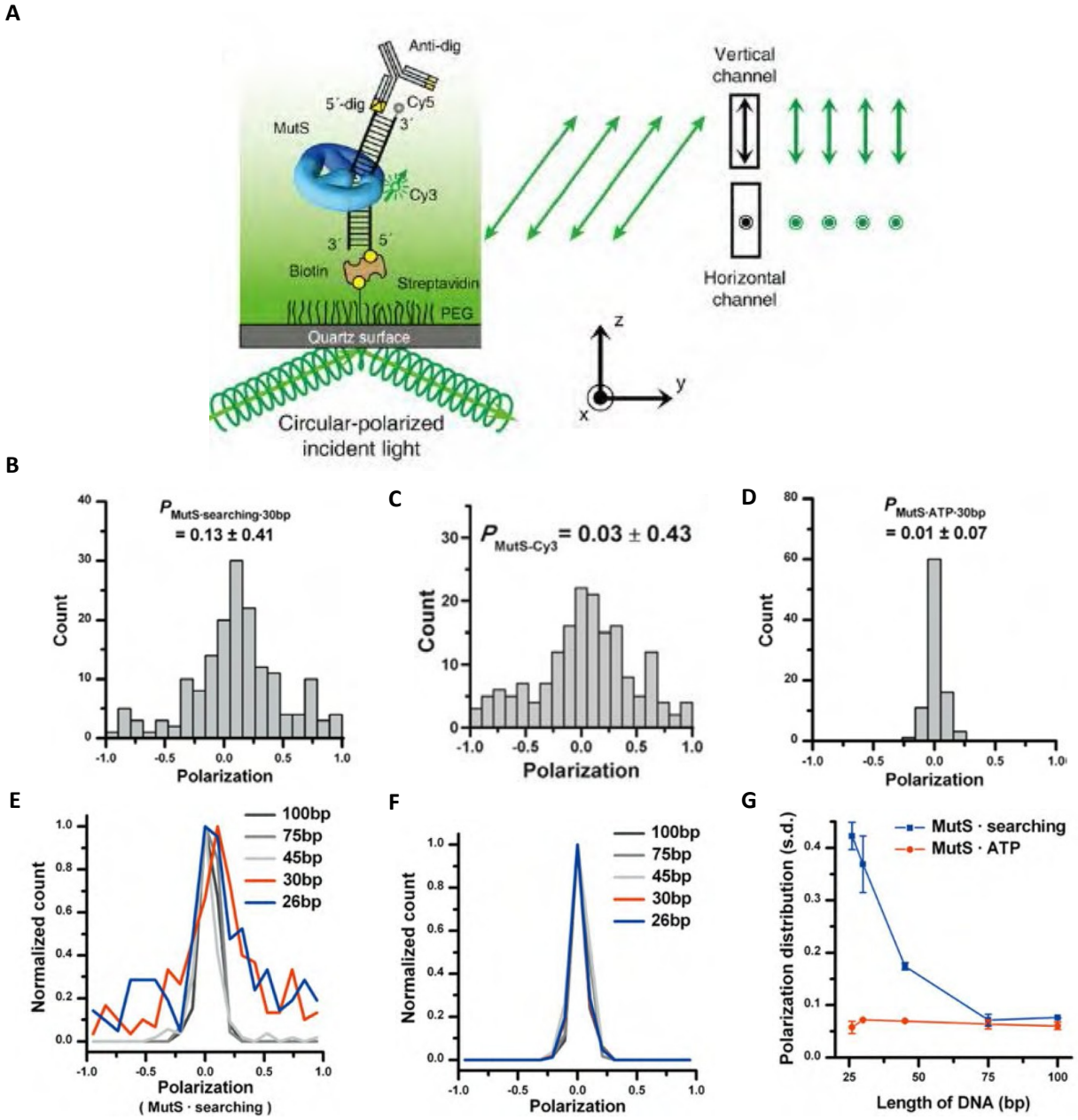

Figure 7. The Rotational Diffusion of MutS along DNA Using smPolarization-TIRF. A. A schematic representation of the smPolarization-TIRF system. A circularly polarized beam, used to excite Cy3-MutS, was colocalized to the DNA via Cy5 emission. The emission polarization directions are defined as a ''horizontal'' polarization (IH) in the plane parallel to the microscope stage and a ''vertical'' polarization (IV) in the plane perpendicular to the microscope stage. **B.** The steady–state polarization of Cy3-MutS nonspecifically immobilized on the surface, which results in the random distribution of the MutS on the surface. The resulting Cy3-MutS polarization is broadly distributed from –1.0 to 1.0. These results indicate that a rigid linkage to the MutS protein suppresses the rotational freedom of the Cy3. **C.** The distribution of polarization of Cy3-MutS restricted by DNA length. ($P_{MutS\cdot searching\cdot 30bp}$ = 0.13 ± 0.41, mean ± s.d.; n = 170). **D.** The distribution of polarization of Cy3-MutS unrestricted by DNA length. ($P_{MutS\cdot mismatch\cdot ATP\cdot 30bp}$ =0.01 ± 0.07, mean ± s.d.; n = 91). **E.** The polarization distributions at various lengths (26, 30, 45, 75, and 100 bp) of duplex DNA. **F.** The polarization distributions at various lengths of duplex DNA containing an unpaired dT mismatch. **G.** The polarization distribution of searching Cy3-MutS and ATP-bound Cy3-MutS at different lengths. Error bars indicate s.e. **(taken from Cho *et al.*, 2012)**

The TACKLE analysis is virtually identical to the kinetic analysis that all FRET-based single molecule laboratories utilize. However, the authors have gone to great lengths to argue that a predominant two-state system (on and off) contains additional separable intermediate states that can be identified by splitting the binned FRET efficiencies of the predominant states into smaller groupings. The demarcation of these FRET groupings appears loosely based on a shift to a slightly higher FRET efficiency for the unbound state in the presence of TaqMutS compared to in the absence of protein. This shift is interpreted as an intermediate kinetic grouping. What is not clear is why that amount of FRET shift difference is used to splay the entire two-state FRET assignments into four additional kinetic states (five if you

include the bound state). There would seem to be several less complicated explanations for the modest FRET shift. First and foremost, the fluorophores are located within the 20-25 bp footprint of the TaqMutS that might influence the searching and binding processes or affect fluorophore quenching. For example, *Jeong et al.,* clearly showed that TaqMutS displays a modest binding efficacy to the fluorophore or its linker on DNA[39]. Perhaps the FRET difference is a result of an altered binding event that is independent of the mismatch but dependent on one or both fluorophores? In addition there is a strand scission near the 5'-acceptor Cy5 that could affect the persistence length when bound by either a searching TaqMutS or a mismatch bound TaqMutS. Any one of these issues or a combination of all might influence the unbound FRET state of the mismatched DNA in the presence of TaqMutS protein. If one exercises Occum's Razor and exploits a single peak FRET state, the lifetime of TaqMutS on a mismatch is ~13s (Table 3). The approximately 3-fold difference in lifetime between these and the *Jeong et al.,* studies[39] could be due to the indirect measure of mismatch binding or the use of a G/T mismatch by *Sass et al.,*[77] that is less well recognized by the TaqMutS than the +T mismatch utilized by *Jeong et al.,*[39].

The smFRET system developed by *Qui et al.,*[78] placed FRET donor (Alexa555) and acceptor (Alexa647) fluorophores within domain I (C42A; M88C) of the TaqMutS that transiently interrogates the mismatch (Fig. 4). As shown by *Jeong et al.,*[39] this is a dangerous place to locate fluorophores because it can affect the activity of TaqMutS. Indeed, there was at least a two-fold difference in ATPase activity with the flourophore labeled protein as measured by bulk pre-steady-state analysis. Maleimide chemistry was used to link the fluorophores to the TaqMutS with the idea that one would partially label the homodimer at one Cys residue with an Alexa555 and the other Cys residue with Alexa647. Based on the labeling efficiency, one can calculate that 28% of the protein preparation had the appropriate combination of Alexa555/Alexa647 FRET pairs. Another 28% of the proteins had both subunits labeled with a single fluorophore and the remaining had either only one subunit labeled (38%) or had no label (6%). The lifetime of TaqMutS on a mismatch was calculated in this system to be just over 2s (Table 3). This lifetime calculation is significantly faster than several other studies (Table 3). It is an interesting coincidence that just over 50% of the proteins have both subunits labeled, and the ATPase activity is reduced by ~50%. This correlation might suggest that a substantial fraction of the TaqMutS used by these investigators was inactive or at the very least displayed altered activity as a result of the labeling procedure. While the idea of examining conformational transitions by smFRET is clearly laudable, one must insure that the FRET visualization method has no effect on protein activity. Unfortunately the nucleotide-binding model building contained in the *Qui et al.,*[78] paper could easily suffer from the biases introduced by the location of the fluorophores. This is especially true when one considers that ATP processing (ATPase) is perhaps the single most important aspect of MSH proteins. The bottom line in this analysis is that while single molecule studies can provide superbly accurate measures, they can also be dramatically influenced by the visualization techniques.

2.2. Mutl Homolog Studies

The function of MLH/PMS proteins in MMR has been enigmatic. Both cellular and biochemical reconstitution studies clearly suggest a central role in licensing the strand scission (*E.coli*) and/or regulating the strand excision process. MLH/PMS proteins contain a GHKL (DNA *G*yrase, *H*sp90, Histidine *K*inase and Mut*L*) ATP binding and hydrolysis motif[79,80]. When bound with ATP, the N-terminal domains of the MLH/PMS homodimer or heterodimer have been suggested to associate (dimerize) with one another[79]. The C-terminal domains of all MLH/PMS proteins have been shown to form stable complexes with their homodimeric or heterodimeric partner[81,82]. The combination of these two observations suggest a homo- or hetero-dimeric protein that has a stable hinge at the C-terminus, a potentially ATP-dependent clasp at the N-terminus, and a large flexible linker between these two domains. Finally, bulk biochemical studies have suggested the MLH/PMS proteins posses an ATP-dependent ssDNA binding activity of unknown function[83-86].

Single molecule analysis of MLH/PMS proteins – In 2010 two papers appeared in the literature that examined activities of single MLH/PMS proteins on DNA[87,88]. *Gorman et al.,* used the DNA curtain smFT system described above, that were modified to contain nanofabricated anchors 15 nm above a passivated surface, to examine the dynamics of ScMlh1-ScPms1[87]. This extraordinary double anchoring method allowed the observation of protein diffusion along the DNA in the absence of hydrodynamic force; a potentially confounding issue in the DNA curtain system (see above). The association of ScMlh1-ScPms1 with duplex DNA was visualized. Remarkably, the diffusion properties appeared consistent with a ring-like architecture that was independent of adenosine nucleotide binding. Moreover, individual ScMlh1-ScPms1 molecules appeared to bypass one another while traveling along the DNA. Because the diffusion coefficient increased with ionic strength, the authors concluded that movement by ScMlh1-ScPms1 occurred by a hopping or stepping mechanism. A polynucleosome array was reconstituted on the DNA curtains where the individual histone octamers that make of the core of reconstituted nucleosomes could be visualized with a qDot-labeled anti-FLAG antibody bound to FLAG-tagged histone H2A. Diffusing ScMlh1-ScPms1 was observed to easily transit nucleosomes suggesting very large hops/steps. The authors then introduced a TEV protease site into the flexible linker region between the C-terminal clasp and the N-terminal GHKL ATPase domains and found that it significantly disrupted the ability of ScMlh1-ScPms1 to associate with the duplex DNA.

Park et al., used an smFRET system to examine ssDNA binding by *E.coli* MutL (EcMutL)[88]. The system employed a short 15bp duplex DNA containing a 33nt oligo-dT tail. A Cy3-donor fluorophore was placed at the end of the ssDNA tail and a Cy5-acceptor fluorophore was placed at the dsDNA-ssDNA junction. In the absence of protein binding the ssDNA would randomly coil in solution placing the Cy3-Cy5 in relatively close proximity and increasing FRET. When bound by an ssDNA binding protein the oligo-dT_{33} will be stretched and the distance between the Cy3-Cy5 will increase, resulting in decreased FRET. Under conditions where bulk ssDNA binding was observed (25 mM salt), the addition of MutL was shown to reduce FRET[88]. FRET reduction was increased ~3-fold in the presence of ATP and mutation of a critical ssDNA binding residue[EcMutL(R266E)] resulted in FRET that was nearly equivalent to the absence of protein. To confirm the FRET studies a single molecule flow-stretching (smFS) analysis was developed where a 5.3 Kb ssDNA was attached to the surface at one end and a 2.8μm polystyrene bead attached to the other end. At a fixed hydrodynamic force that was controlled by laminar flow rate, the bead position was fixed and dependent on the retraction forces associated with the random coil of ssDNA. Binding EcMutL uncoils the ssDNA extending the position of the bead in the laminar flow. These studies confirmed EcMutL ssDNA binding, but demonstrated that the binding/extension activity decreased to zero at 120 mM salt.

Combining the *Gorman et al.,*[73] and *Park et al.,*[88] single molecule studies has begun to illuminate MLH/PMS function(s). One seeming contradiction is that *Park et al.,*[88] observed essentially no ssDNA binding/extension at 120 mM salt, while *Gorman et al.,* observed relatively stable dsDNA binding and step/hop diffusion in 150 mM salt. These observations might be reconciled if one hypothesizes that both DNA binding domains of the homo-/hetero-dimer located in the flexible linker must associate with the DNA for binding/extension, while only one is required for step/hop diffusion. In such a case, increasing salt would affect the lifetime and dynamics of each binding domain independently ultimately increasing the probability that one will dissociate in the time frame of the smFS analysis. At physiological salt, the MLH/PMS would appear to form some type of very large and flexible clamp that may step/hop using alternate DNA binding domains but is incapable of stably binding/stretching the DNA. Interestingly, later smFT DNA curtain studies appear to suggest that step/hop-diffusing ScMlh1-ScPms1 strongly associates with ATP-bound ScMsh2-ScMsh6 sliding clamps (i.e. it does not step/hop over the ScMsh2-ScMsh6)[73]. These observations are clearly intriguing and require additional single molecule and/or FRET analysis.

Although the *Gorman et al.,*[73] and *Park et al.,*[88] single molecule studies have opened the door for investigating the cryptic behaviors of MLH/PMS proteins, several questions remain: 1.) what kind of specific interactions occur between the sliding complex of MSH and MLH/PMS and downstream partners to elicit DNA excision, 2.) when and how is the MLH/PMS endonuclease activated, 3.) what is the specific role of multiple MSH-MLH/PMS sliding clamp complexes, 4.) What happens to the MLH/PMS structure when it associates with the ATP-bound MSH sliding clamp, among others.

In addition to these MMR questions, there are also basic biophysical questions. The *Gorman et al.,*[73] studies suggest that the sliding complex containing ScMsh2-ScMsh6/ScMlh1-ScPms1 display a similar dwelling time and a faster diffusion coefficient than ScMSh2-ScMsh6 alone. The similar dwell time might be explained if there is occlusion of the ScMlh1-ScPms2 DNA binding site(s) by the ScMsh2-ScMsh6/ScMlh1-ScPms1 complex. However, a faster diffusion coefficient is opposite to what one would expect for the diffusion of a larger complex with a larger surface area exposed to the viscous solution. Clearly, quantitative smFRET/FT analysis will help to resolve these issues.

3. Technical Development Required for FRET Analysis of MMR

The ultimate goal of the MMR single molecule FRET studies is the visualization of the complete reaction in both the prokaryotic and eukaryotic systems. Part and parcel to this goal is the analysis of individual protein-protein interactions that occur during MMR. The latter studies appear more technically feasible with present-day technologies since many of these are simple two-component interactions. However, if one is to use smFRET/FT as a method of visualization, a much less obtrusive method for fluorophore labeling will be required than the use of qDot-labeled antibodies. This issue underlines several technical issues that need to be addressed in the development of MMR single molecule studies that include: 1.) Fluorophore labeling of proteins, 2.) Spatial resolution as it applies to the co-localization of protein-protein and protein-DNA interactions, 3.) Rectifying different results from different laboratories, and 4.) Constructing appropriate DNA substrates and visualizing them in an appropriate single molecule apparatus.

3.1. Fluorophore Labeling of Proteins

The first technical issue is fluorophore labeling of proteins for smFRET/FT analysis. A number of methods have been developed for protein labeling by researchers working in chemistry, biochemistry and biophysics. These methods can be broadly broken down into two major groups: 1.) introduction of specific amino acid modifications amenable to chemical labeling, and 2.) addition of peptide fusion tags. Amino acid modifications include cysteine introduction/ deletion, amine group modifications, and non-natural amino acids incorporation. The addition of peptide fusion tags include fluorescent proteins (GFP, RFP, etc.,), Halo(haloalkane dehalogenase)-Tag, SNAP/CLIP

(O^6-alkylguanine-DNA alkyltransferase)-Tag, Avi(biotin ligase recognition peptide)-Tag, Sfp phosphopantetheinyl transferase(CoA)-Tag, and FGE(formylglycine generating enzyme recognition peptide)-Tag. Each of these labeling technologies have both advantages and disadvantages.

Amino acid modification - One of the most common labeling methods is the conjugation of a thiol-reactive group (such as maleimide-fluorophore) to a solvent-accessible cysteine in the protein. For the smFRET/FT studies described above, TaqMutS was labeled by this method [36,39,78,89]. However, if the protein contains multiple cysteine residues, then site-directed mutagenesis must be performed to replace them. For the vast majority of proteins cysteine labeling is not a viable option either due to excessive cysteine residues or the lack of sufficient structural information required to generate 'Cys light' substitution mutations.

Amine groups may also be exploited for their ability to react with some amine-reactive reagents (such as succinimidyl esters). Unfortunately, this method often results in multiple labeling events per protein because of the high frequency of lysine and arginine residues. Specific modification of the N-terminal α-amine group with succinimidyl ester conjugates because of their low pK_a has been reported[90,91]. However, a recent publication pointed out that the specificity of this method might be less than 40%[92].

The incorporation of non-natural amino acids is another method to label proteins. Modified aminoacyl tRNA synthetases have been developed to incorporate non-natural amino acids (some containing a fluorophore) into a growing peptide chain via specific codon recognition. These codons only exist in the proteins of interest so that the labeling is specific. This method has been used for protein labeling studies *in vivo*[93]. However, the incorporation efficiency of the non-natural amino acid appears to be quite low *in vivo*, such that a cell-free protein synthesis system is often utilized[94]. In spite of the fact that single molecule analysis requires very little fluorophore-labeled protein compared to bulk studies, it appears that the non-natural amino acid incorporation methodology rarely produces sufficient quantities of protein for an accurate determination.

Fusion Protein/Peptides – The fusion of a fluorescent protein has been a staple of protein visualization for over two decades[95]. Since the use of green fluorescent protein (GFP) as a bio-marker, other fluorescent mutants (such as YFP, CFP) have been constructed.[96]. These multiple fluorescent protein derivatives display different excitation/emission spectra and relatively strong photostability, which ultimately makes them useful in FRET and single molecule experiments. There are numerous examples of single molecule imaging studies using GFP-protein fusions *in vivo* (see for example:[97,98]. However, GFP and its derivatives are large peptides (~27kD) that may interfere with the function and/or interaction(s) of the protein under study. In addition, GFP derivatives may form oligomers that could introduce serious artifacts[96].

The Halo-Tag method employs the haloalkane dehalogenase protein (33kD) where a catalytic triad mutation produces an irreversible covalent link between a fluorophore-modified ligand and the protein[99,100]. Commercially available Halo-Tag ligands labeled with coumarin and fluorescein are presently available. The large size of the haloalkane dehalogenase protein fusion may have similar deficiencies to the GFP derivatives described above.

The SNAP-tag (20kD) and CLIP-tag (21KD) are labeling systems based on human O^6-alkylguanine-DNA alkyltransferase (hAGT). The hAGT catalyzes auto-modification with an alkyl group from its natural substrate O^6-alkylguanine or a benzylguanine[101]. There are several commercially available substates which fluorophores, biotin or beads conjugated to benzylguanine (SNAP-tag) or benzylcytosine (CLIP-tag). However, here again the large size of the O^6-alkylguanine-DNA alkyltransferase protein fusion may have similar deficiencies to the GFP derivatives described above.

Biotinylation has become a useful method to label, purify, or immobilize proteins. In contrast to chemical biotinylation methods, enzymatic biotinylation allows biotin to be linked to exactly one residue present in the protein. The fusion of a fifteen amino acid peptide (Avi-Tag) to the protein of interest provides a specific site for enzymatic biotinylation. The tagged protein may then be incubated with purified biotin ligase (BirA) in the presence of biotin and ATP *in vitro*, or co-expressed with the BirA gene *in vivo* to produce a protein with a single specific biotin residue[102,103]. A biotinylated-protein may then be labeled with a fluorescent streptavidin (53kD) or a fluorescent qDot linked to streptavidin (>53kD). Biotinylated proteins are extremely rare in nature, making the chances for cross-reactivity very low. The shortcoming of this method is that the size of the conjugated complex may be too large (>15nm) for most proteins (see above). However, biotinylation is clearly a viable method for the immobilization of proteins on a single molecule surface.

A small tetracysteine tag has also been used for protein labeling[104,105]. The tetracysteine binding-motif contains six amino acids (CCXXCC), which in most cases is unlikely to disrupt native protein function. Invitrogen currently markets fluorescent molecules that may be specifically linked to the tetracysteine tag. However, non-specific binding of the fluorescent molecules to other cysteine rich motifs makes this approach unsuitable for many single molecule applications[106,107].

Sfp phosphopantetheinyl transferase recognizes the ybbR tag (eleven amino acids) and will transfer a 4'-phos-phopantetheinyl group from CoA to a serine residue in the tag[108,109]. Proteins with ybbR tags can be specifically labeled using fluorescent CoA. SFP Synthase and fluorescent CoA (CoA-488, CoA-547 and CoA647) are now available from New England Biolabs, and several single molecule studies have used this method[110-113]. One drawback of this method is the labeling efficiency. Unlike the FGE method in which tag modification and tag labeling

are two distinct steps, this labeling protocol is done in one intricate step. The requirement that the modification be done *in vitro* and at low temperature makes for difficult enzymology. Moreover, the reported labeling to date is 17% after 24h[110].

Formylglycine generating enzyme (FGE) catalyzes the formation of a formylglycine residue from a central cysteine in a highly conserved six amino acid motif (LCTPSR; [92,114,115]. The formylglycine post-translational modification may be introduced *in vivo* by co-expression of FGE or *in vitro* using purified FGE protein[92,114,115]. Aminooxy- or hydrazide-functionalized probes may be conjugated to the aldehyde group of formylglycine. The reaction is specific as there are very few aldehyde groups in naturally occurring amino acids. It has been reported that 100% protein labeling can be obtained using this method, and is suitable for single molecule experiments[92]. The shortcoming of this method is that a large amount of dye must be used[92] and the spontaneous reversibility of the hydrozone linkage[116].

These labeling methods present many opportunities for measuring proteins in smFRET/FT systems. Specific labeling is particularly important for smFRET, in which two fluorophores at defined distance are required. Although it is possible to purify and dual-label proteins *in vitro*, many problems still remain with the labeling methods themselves. A new method that has higher efficiency, greater specificity, and does not interfere with normal protein function, would greatly expand the application of single molecule experiments in biological events.

3.2. Spatial Resolution and Co-localization of Interactions

Monitoring multiple proteins simultaneously and eventually the entire MMR process presents significant resolution challenges. Because the spatial resolution of smFRET/FT is diffraction limited (~200-300nm) and the typical footprint of an MSH is about 10-20nm, it is possible that there may be over 10 ATP-bound MSH sliding clamps in one florescent spot recorded by the CCD camera. *Gorman et al.,*[75] found that with a fixed Qdot the standard deviation was about +/- 16nm with a 2D Gaussian peak analysis of a fluorescent spot in the DNA curtain smFT[75]. However, as a result of the fluctuating nature of long DNAs in smFT, proteins in thermal motion and the properties of the fluorophore, it is inferred that the spatial resolution is likely to easily exceed 20nm; even from the 2D Gaussian peak analysis where there may be several MSH molecules in one spot. These observations are likely to cloud any conclusions whether a protein-protein interaction on an smFT DNA is coincident or specific. Several schemes have been devised to overcome this obstacle. For example, bleaching fluorophores to count the number of molecules, measuring speed, observing collision, and designing multiple FRET pairs.

Super resolution microscopy that resolves single molecules below the diffraction limit has begun to come of age using RapidSTORM (Neubeck& Van Gool algorithm) [117], QuickPALM (classical Högbom 'CLEAN' algorithm) [118], LivePALM (fluoroBancroft algorithm) [119], radial symmetry centers[120] or Maximum Likelihood Estimation (MLE) algorithms[121] to localize particles. Most supper resolution studies have required fixed samples since the number of photons is usually quite low and any molecular movement (diffusion) would influence the acquisition algorithms ultimately decreasing the special resolution. Work on feed back mechanisms that rely on parallel localization processing continues to show promise for super resolution of particle locaization in real time[122].

3.3. Variation in the Quantitative Analysis between Multiple Laboratories

The differences in quantitative analysis between laboratories are most clearly demonstrated in Table 3. It might be argued that differences between TaqMutS and ScMsh2-ScMsh6 could be explained by the size differences and the nature of the complex (homodimer vs. heterodimer). However, the wide range of measures, even between different TaqMutS studies is disturbing. There are some factors that might have affected results that include the use of a relatively strong flow and the use of differing ionic conditions. Careful comparison of experimental procedures and designs might explain some if not all of the disagreements. One issue that would clearly help to mollify differences would be to insist that single molecule studies be performed under physiologically relevant ionic conditions.

3.4. Construction of Appropriate DNA Substrates and Visualization

The cellular process of MMR occurs on DNA with mismatches, nicks, gaps and/or methylated sites for *E.coli* as well as in the presence of fully or partially reconstituted chromatin. Due to the spatial resolution problem a long DNA is required to observe a complete process. However, it is not a simple task to construct a DNA that is over 10kb and containing a single mismatch. Moreover, before and after the actual single molecule experiment, it is necessary to confirm the status of a long DNA since they are relatively fragile in a flow system. Sytox staining has been typically used to confirm nature of the DNA on a single molecule surface [123]. However, when examining DNA repair proteins that recognize lesions in the DNA, it is important to determine that residual visualizing reagent does not interfere with the observations. Despite these obstacles smFRET/FT studies of MMR components have been successful. There is no doubt that with some small improvements, the smFRET/FT methods will become more promising schemes in studying MMR.

4. Concluding Remarks

FRET studies have played an important role in detailing

the interactions and kinetics of MMR proteins on mismatched DNA. Careful design of FRET donor and acceptor locations is essential to insure accuracy as well as a lack of influence on biological functions. We have provided several examples where the lack of careful attention to biophysical details has likely led to dramatic overinterpretation of the data and models with almost no biological relevance. Clearly the development of labeling technologies and new quantitative analysis will lead to further understanding of the biophysics of MMR. In addition, the development of real-time cellular single molecule analysis where FRET plays an integral role in determining interactions and positioning is on the horizon.

ACKNOWLEDGEMENTS

The authors would like to thank members of the Lee and Fishel laboratories for helpful discussions. This work was supported by the National Research Foundation (NRF) of Korea and the Ministry of Education, Science, and Technology (MEST; 2011-0013901; J-BL) and NIH grant CA67007 (RF).

REFERENCES

[1] E.M. Witkin Pure clones of lactose negative mutants obtained in Escherichia coli after treatment with 5-bromouracil, J. Mol. Biol. 8 (1964) 610-613.

[2] R.A. Holliday A mechanism for gene conversion in fungi, Genet. Res. 5 (1964) 282-304.

[3] M. Roger Evidence for conversion of heteroduplex transforming DNAs to homoduplex by recipient pneumococcal cells, Proc. Nat. Acad. Sci. (USA) 69 (1972) 466-470.

[4] J.-G. Tiraby and M.S. Fox Marker discrimination in transformation and mutation of pneumococcus, Proc. Natl. Acad. Sci. U. S. A. 70 (1973) 3541-3545.

[5] S. Acharya and R. Fishel The mechanism of DNA mismatch repair from bacteria to human, Taylor & Francis Group, New Yok, NY, 2006.

[6] J. Jiricny The multifaceted mismatch-repair system, Nat Rev Mol Cell Biol 7 (2006) 335-346.

[7] R.D. Kolodner and G.T. Marsischky Eukaryotic DNA mismatch repair.[Review][84 refs], Current Opinion in Genetics & Development 9 (1999) 89-96.

[8] P. Modrich Strand-specific mismatch repair in mammalian cells[Review], Journal of Biological Chemistry 272 (1997) 24727-24730.

[9] C. Rayssiguier, D.S. Thaler and M. Radman The barrier to recombination between Escherichia coli and Salmonella typhimurium is disrupted in mismatch-repair mutants, Nature 342 (1989) 396-401.

[10] R. Fishel The selection for mismatch repair defects in hereditary nonpolyposis colorectal cancer: revising the mutator hypothesis, Cancer Research 61 (2001) 7369-7374.

[11] J.G. Gong, A. Costanzo, H.Q. Yang, G. Melino, W.G. Kaelin, Jr., M. Levrero and J.Y. Wang The tyrosine kinase c-Abl regulates p73 in apoptotic response to cisplatin-induced DNA damage[see comments], Nature 399 (1999) 806-809.

[12] H. Zhang, B. Richards, T. Wilson, M. Lloyd, A. Cranston, A. Thorburn, R. Fishel and M. Meuth Apoptosis induced by overexpression of hMSH2 or hMLH1, Cancer Research 59 (1999) 3021-3027.

[13] C.E. Bronner, S.M. Baker, P.T. Morrison, G. Warren, L.G. Smith, M.K. Lescoe, M. Kane, C. Earabino, J. Lipford, A. Lindblom and et al. Mutation in the DNA mismatch repair gene homologue hMLH1 is associated with hereditary non-polyposis colon cancer, Nature 368 (1994) 258-261.

[14] R. Fishel, M.K. Lescoe, M.R. Rao, N.G. Copeland, N.A. Jenkins, J. Garber, M. Kane and R. Kolodner The human mutator gene homolog MSH2 and its association with hereditary nonpolyposis colon cancer, Cell 75 (1993) 1027-1038.

[15] F.S. Leach, N.C. Nicolaides, N. Papadopoulos, B. Liu, J. Jen, R. Parsons, P. Peltomaki, P. Sistonen, L.A. Aaltonen, M. Nystrom-Lahti, X.-Y. Guan, J. Zhang, P.S. Meltzer, J.-W. Yu, F.-T. Kao, D.J. Chen, K.M. Cerosaletti, R.E.K. Fournier, S. Todd, T. Lewis, R.J. Leach, S.L. Naylor, J. Weissenbach, J.-P. Mecklin, H. Jarvinen, G.M. Petersen, S.R. Hamilton, J. Green, J. Jass, P. Watson, H.T. Lynch, J.M. Trent, A. de la Chapelle, K.W. Kinsler and B. Vogelstein Mutations of a mutS Homolog in Hereditary Nonpolyposis Colorectal Cancer, Cell 75 (1993) 1215-1225.

[16] N.C. Nicolaides, N. Papadopoulos, B. Liu, Y.F. Wei, K.C. Carter, S.M. Ruben, C.A. Rosen, W.A. Haseltine, R.D. Fleischmann, C.M. Fraser and et al. Mutations of two PMS homologues in hereditary nonpolyposis colon cancer, Nature 371 (1994) 75-80.

[17] N. Papadopoulos, N.C. Nicolaides, B. Liu, R. Parsons, C. Lengauer, F. Palombo, A. D'Arrigo, S. Markowitz, J.K.V. Willson, K.W. Kinzler, J. Jiricny and B. Vogelstein Mutations of GTBP in genetically unstable cells, Science 268 (1995) 1915-1917.

[18] N. Papadopoulos, N.C. Nicolaides, Y.-F. Wei, S.M. Ruben, K.C. Carter, C.A. Rosen, W.A. Haseltine, R.D. Fleischmann, C.M. Fraser, M.D. Adams, J.C. Venter, S.R. Hamilton, G.M. Petersen, P. Watson, H.T. Lynch, P. Peltomaki, J.-P. Mecklin, A. de la Chapelle, K.W. Kinzler and B. Vogelstein Mutation of a mutL Homolog in Hereditary Colon Cancer, Science 263 (1994) 1625-1629.

[19] M. Demerec, E.L. Lahr, T. Miyake, E. Galehran, E. Balbinder, S. Baric, K. Hashimoto, E.V. Glanville and J.D. Gross Bacterial Genetics, Carnegie Inst. Wash. Yearbook 370 (1957) 390-406.

[20] R.F. Hill Location of genes controlling excision repair of UV damage and mutator activity in Escherichia coli WP2, Mutat. Res. 9 (1970) 341-344.

[21] E.C. Siegel and V. Bryson Mutator Gene of Escherichia coli B, J. Bacteriol. 94 (1967) 38-47.

[22] J.V. Martin-Lopez and R. Fishel The mechanism of mismatch repair and the functional analysis of mismatch repair defects in Lynch syndrome, Fam Cancer (2013).

[23] S.-S. Su and P. Modrich Escherichia coli mutS-encoded protein binds to mismatched DNA base pairs, Proc. Natl. Acad. Sci. U. S. A. 83 (1986) 5057-5061.

[24] S. Acharya, T. Wilson, S. Gradia, M.F. Kane, S. Guerrette, G.T. Marsischky, R. Kolodner and R. Fishel hMSH2 forms specific mispair-binding complexes with hMSH3 and hMSH6, Proc Natl Acad Sci U S A 93 (1996) 13629-13634.

[25] T. Bocker, A. Barusevicius, T. Snowden, D. Rasio, S. Guerrette, D. Robbins, C. Schmidt, J. Burczak, C.M. Croce, T. Copeland, A.J. Kovatich and R. Fishel hMSH5: a human MutS homologue that forms a novel heterodimer with hMSH4 and is expressed during spermatogenesis, Cancer Research 59 (1999) 816-822.

[26] R. Fishel and T. Wilson MutS homologs in mammalian cells.[Review][84 refs], Curr Opin Genet Dev 7 (1997) 105-113.

[27] S. Gradia, S. Acharya and R. Fishel The role of mismatched nucleotides in activating the hMSH2-hMSH6 molecular switch, J. Biol. Chem. 275 (2000) 3922-3930.

[28] J.M. Harrington and R.D. Kolodner Saccharomyces cerevisiae Msh2-Msh3 acts in repair of base-base mispairs, Mol Cell Biol 27 (2007) 6546-6554.

[29] G.T. Marsischky, N. Filosi, M.F. Kane and R. Kolodner Redundancy of saccharomyces cerevisiae MSH3 and MSH6 in MSH2-dependent mismatch repair, Genes & Development 10 (1996) 407-420.

[30] T. Wilson, S. Guerrette and R. Fishel Dissociation of mismatch recognition and ATPase activity by hMSH2-hMSH3, J. Biol. Chem. 274 (1999) 21659-21644.

[31] M.H. Lamers, A. Perrakis, J.H. Enzlin, H.H. Winterwerp, N. de Wind and T.K. Sixma The crystal structure of DNA mismatch repair protein MutS binding to a G x T mismatch.[see comments], Nature 407 (2000) 711-717.

[32] G. Obmolova, C. Ban, P. Hsieh and W. Yang Crystal structures of mismatch repair protein MutS and its complex with a substrate DNA.[see comments], Nature 407 (2000) 703-710.

[33] C.D. Heinen, J.L. Cyr, C. Cook, N. Punja, M. Sakato, R.A. Forties, J.M. Lopez, M.M. Hingorani and R. Fishel Human MSH2 (hMSH2) protein controls ATP processing by hMSH2-hMSH6, J Biol Chem 286 (2011) 40287-40295.

[34] M.H. Lamers, H.H. Winterwerp and T.K. Sixma The alternating ATPase domains of MutS control DNA mismatch repair, Embo J 22 (2003) 746-756.

[35] S. Acharya, P.L. Foster, P. Brooks and R. Fishel The coordinated functions of the E. coli MutS and MutL proteins in mismatch repair, Molecular Cell. 12 (2003) 233-246.

[36] W.K. Cho, C. Jeong, D. Kim, M. Chang, K.M. Song, J. Hanne, C. Ban, R. Fishel and J.B. Lee ATP alters the diffusion mechanics of MutS on mismatched DNA, Structure 20 (2012) 1264-1274.

[37] S. Gradia, S. Acharya and R. Fishel The human mismatch recognition complex hMSH2-hMSH6 functions as a novel molecular switch, Cell 91 (1997) 995-1005.

[38] S. Gradia, D. Subramanian, T. Wilson, S. Acharya, A. Makhov, J. Griffith and R. Fishel hMSH2-hMSH6 forms a hydrolysis-independent sliding clamp on mismatched DNA, Molecular Cell 3 (1999) 255-261.

[39] C. Jeong, W.K. Cho, K.M. Song, C. Cook, T.Y. Yoon, C. Ban, R. Fishel and J.B. Lee MutS switches between two fundamentally distinct clamps during mismatch repair, Nat Struct Mol Biol 18 (2011) 379-385.

[40] M. Grilley, K.M. Welsh, S.S. Su and P. Modrich Isolation and characterization of the Escherichia coli mutL gene product, J Biol Chem 264 (1989) 1000-1004.

[41] M.G. Marinus Methylation of prokaryotic DNA, in: A. Razin, H. Cedar and A.D. Riggs (Eds.), DNA Methylation, Biochemistry and Biological Significance, Springer-Verlag, New York, 1984, pp. 81-109.

[42] K.M. Welsh, A.L. Lu, S. Clark and P. Modrich Isolation and characterization of the Escherichia coli mutH gene product, J Biol Chem 262 (1987) 15624-15629.

[43] M. Viswanathan and S.T. Lovett Single-strand DNA-specific exonucleases in Escherichia coli - roles in repair and mutation avoidance, Genetics 149 (1998) 7-16.

[44] N. Constantin, L. Dzantiev, F.A. Kadyrov and P. Modrich Human mismatch repair: reconstitution of a nick-directed bidirectional reaction, J Biol Chem 280 (2005) 39752-39761.

[45] M. Grilley, J. Griffith and P. Modrich Bidirectional excision in methyl-directed mismatch repair, J Biol Chem 268 (1993) 11830-11837.

[46] R.S. Lahue, K.G. Au and P. Modrich DNA mismatch correction in a defined system, Science 245 (1989) 160-164.

[47] R.D. Kolodner, M.L. Mendillo and C.D. Putnam Coupling distant sites in DNA during DNA mismatch repair, Proc Natl Acad Sci U S A 104 (2007) 12953-12954.

[48] M.S. Junop, G. Obmolova, K. Rausch, P. Hsieh and W. Yang Composite active site of an ABC ATPase: MutS uses ATP to verify mismatch recognition and authorize DNA repair, Molecular Cell 7 (2001) 1-12.

[49] D.J. Allen, A. Makhov, M. Grilley, J. Taylor, R. Thresher, P. Modrich and J.D. Griffith MutS mediates heteroduplex loop formation by a translocation mechanism, EMBO Journal 16 (1997) 4467-4476.

[50] L.J. Blackwell, K.P. Bjornson and P. Modrich DNA-dependent activation of the hMutS alpha ATPase, Journal of Biological Chemistry 273 (1998) 32049-32054.

[51] R. Fishel, S. Acharya, M. Berardini, T. Bocker, N. Charbonneau, A. Cranston, S. Gradia, S. Guerrette, C.D. Heinen, A. Mazurek, T. Snowden, C. Schmutte, K.-S. Shim, G. Tombline and T. Wilson Signaling Mismatch Repair: the mechanics of an adenosine-nucleotide molecular switch, Cold Spring Harbor Symp. Quant. Biol. 65 (2000) 217-224.

[52] A. Pluciennik and P. Modrich Protein roadblocks and helix discontinuities are barriers to the initiation of mismatch repair, Proc Natl Acad Sci U S A 104 (2007) 12709-12713.

[53] R. Fishel Mismatch repair, molecular switches, and signal transduction.[Review][56 refs], Genes & Development 12

(1998) 2096-2101.

[54] Y. Zhang, F. Yuan, S.R. Presnell, K. Tian, Y. Gao, A.E. Tomkinson, L. Gu and G.M. Li Reconstitution of 5'-directed human mismatch repair in a purified system, Cell 122 (2005) 693-705.

[55] L. Dzantiev, N. Constantin, J. Genschel, R.R. Iyer, P.M. Burgers and P. Modrich A defined human system that supports bidirectional mismatch-provoked excision, Mol Cell 15 (2004) 31-41.

[56] C. Schmutte, R.C. Marinescu, M.M. Sadoff, S. Guerrette, J. Overhauser and R. Fishel Human exonuclease I interacts with the mismatch repair protein hMSH2, Cancer Research 58 (1998) 4537-4542.

[57] D.X. Tishkoff, N.S. Amin, C.S. Viars, K.C. Arden and R.D. Kolodner Identification of a human gene encoding a homologue of Saccharomyces cerevisiae EXO1, an exonuclease implicated in mismatch repair and recombination, Cancer Research 58 (1998) 5027-5031.

[58] D.X. Tishkoff, A.L. Boerger, P. Bertrand, N. Filosi, G.M. Gaida, M.F. Kane and R.D. Kolodner Identification and characterization of Saccharomyces cerevisiae EXO1, a gene encoding an exonuclease that interacts with MSH2, Proceedings of the National Academy of Sciences of the United States of America 94 (1997) 7487-7492.

[59] F.A. Kadyrov, L. Dzantiev, N. Constantin and P. Modrich Endonucleolytic function of MutLalpha in human mismatch repair, Cell 126 (2006) 297-308.

[60] F.A. Kadyrov, S.F. Holmes, M.E. Arana, O.A. Lukianova, M. O'Donnell, T.A. Kunkel and P. Modrich Saccharomyces cerevisiae MutLalpha is a mismatch repair endonuclease, J Biol Chem 282 (2007) 37181-37190.

[61] M.C. Pillon, J.J. Lorenowicz, M. Uckelmann, A.D. Klocko, R.R. Mitchell, Y.S. Chung, P. Modrich, G.C. Walker, L.A. Simmons, P. Friedhoff and A. Guarne Structure of the endonuclease domain of MutL: unlicensed to cut, Mol Cell 39 (2010) 145-151.

[62] M.C. Pillon, J.H. Miller and A. Guarne The endonuclease domain of MutL interacts with the beta sliding clamp, DNA Repair (Amst) 10 (2011) 87-93.

[63] N.S. Amin, M.N. Nguyen, S. Oh and R.D. Kolodner exo1-Dependent mutator mutations: model system for studying functional interactions in mismatch repair, Mol Cell Biol 21 (2001) 5142-5155.

[64] K. Wei, A.B. Clark, E. Wong, M.F. Kane, D.J. Mazur, T. Parris, N.K. Kolas, R. Russell, H. Hou, Jr., B. Kneitz, G. Yang, T.A. Kunkel, R.D. Kolodner, P.E. Cohen and W. Edelmann Inactivation of Exonuclease 1 in mice results in DNA mismatch repair defects, increased cancer susceptibility, and male and female sterility, Genes Dev 17 (2003) 603-614.

[65] N. Sugawara, T. Goldfarb, B. Studamire, E. Alani and J.E. Haber Heteroduplex rejection during single-strand annealing requires Sgs1 helicase and mismatch repair proteins Msh2 and Msh6 but not Pms1, Proc Natl Acad Sci U S A 101 (2004) 9315-9320.

[66] B.D. Harfe and S. Jinks-Robertson DNA mismatch repair and genetic instability, Annu Rev Genet 34 (2000) 359-399.

[67] L. Worth, Jr., S. Clark, M. Radman and P. Modrich Mismatch repair proteins MutS and MutL inhibit RecA-catalyzed strand transfer between diverged DNAs, Proc Natl Acad Sci U S A 91 (1994) 3238-3241.

[68] R. Fishel Signaling mismatch repair in cancer, Nature Medicine 5 (1999) 1239-1241.

[69] K. Yoshioka, Y. Yoshioka and P. Hsieh ATR kinase activation mediated by MutSalpha and MutLalpha in response to cytotoxic O6-methylguanine adducts, Mol Cell 22 (2006) 501-510.

[70] P. Peltomaki and H. Vasen Mutations associated with HNPCC predisposition -- Update of ICG-HNPCC/INSiGHT mutation database, Dis Markers 20 (2004) 269-276.

[71] L.A. Loeb Mutator phenotype may be required for multistage carcinogenesis.[Review][63 refs], Cancer Res 51 (1991) 3075-3079.

[72] D.P. Lin, Y. Wang, S.J. Scherer, A.B. Clark, K. Yang, E. Avdievich, B. Jin, U. Werling, T. Parris, N. Kurihara, A. Umar, R. Kucherlapati, M. Lipkin, T.A. Kunkel and W. Edelmann An Msh2 point mutation uncouples DNA mismatch repair and apoptosis, Cancer Res 64 (2004) 517-522.

[73] J. Gorman, F. Wang, S. Redding, A.J. Plys, T. Fazio, S. Wind, E.E. Alani and E.C. Greene Single-molecule imaging reveals target-search mechanisms during DNA mismatch repair, Proc Natl Acad Sci U S A 109 (2012) E3074-3083.

[74] R. Roy, S. Hohng and T. Ha A practical guide to single-molecule FRET, Nat Methods 5 (2008) 507-516.

[75] J. Gorman, A. Chowdhury, J.A. Surtees, J. Shimada, D.R. Reichman, E. Alani and E.C. Greene Dynamic basis for one-dimensional DNA scanning by the mismatch repair complex Msh2-Msh6, Mol Cell 28 (2007) 359-370.

[76] O.G. Berg, R.B. Winter and P.H. von Hippel Diffusion-driven mechanisms of protein translocation on nucleic acids. 1. Models and theory, Biochemistry 20 (1981) 6929-6948.

[77] L.E. Sass, C. Lanyi, K. Weninger and D.A. Erie Single-molecule FRET TACKLE reveals highly dynamic mismatched DNA-MutS complexes, Biochemistry 49 (2011) 3174-3190.

[78] R. Qiu, V.C. DeRocco, C. Harris, A. Sharma, M.M. Hingorani, D.A. Erie and K.R. Weninger Large conformational changes in MutS during DNA scanning, mismatch recognition and repair signalling, Embo J 31 (2012) 2528-2540.

[79] C. Ban and W. Yang Crystal structure and ATPase activity of MutL: Implications for DNA repair and mutagenesis, Cell 95 (1998) 541-552.

[80] R. Dutta and M. Inouye GHKL, an emergent ATPase/kinase superfamily, Trends in Biochemical Sciences 25 (2000) 24-28.

[81] N. Charbonneau, R. Amunugama, C. Schmutte, K. Yoder and R. Fishel Evidence that hMLH3 functions primarily in meiosis and in hMSH2-hMSH3 mismatch repair, Cancer Biol Ther 8 (2009) 1411-1420.

[82] S. Guerrette, S. Acharya and R. Fishel The interaction of the human MutL homologues in hereditary nonpolyposis colon cancer, J Biol Chem 274 (1999) 6336-6341.

[83] C. Ban, M. Junop and W. Yang Transformation of MutL by ATP binding and hydrolysis: a switch in DNA mismatch repair, Cell 97 (1999) 85-97.

[84] S.M. Bende and R.H. Grafstrom The DNA binding properties of the MutL protein isolated from Escherichia coli, Nucleic Acids Res. 19 (1991) 1549-1555.

[85] M.C. Hall, H. Wang, D.A. Erie and T.A. Kunkel High Affinity Cooperative DNA Binding by the Yeast Mlh1-Pms1 Heterodimer, J. Mol. Biol 312 (2001) 637-647.

[86] A. Robertson, S.R. Pattishall and S.W. Matson The DNA binding activity of MutL is required for methyl-directed mismatch repair in Escherichia coli, J Biol Chem 281 (2006) 8399-8408.

[87] J. Gorman, A.J. Plys, M.L. Visnapuu, E. Alani and E.C. Greene Visualizing one-dimensional diffusion of eukaryotic DNA repair factors along a chromatin lattice, Nat Struct Mol Biol 17 (2010) 932-938.

[88] J. Park, Y. Jeon, D. In, R. Fishel, C. Ban and J.B. Lee Single-molecule analysis reveals the kinetics and physiological relevance of MutL-ssDNA binding, PLoS One 5 (2010) e15496.

[89] L.E. Sass, C. Lanyi, K. Weninger and D.A. Erie Single-molecule FRET TACKLE reveals highly dynamic mismatched DNA-MutS complexes, Biochemistry 49 (2010) 3174-3190.

[90] R. Galletto, I. Amitani, R.J. Baskin and S.C. Kowalczykowski Direct observation of individual RecA filaments assembling on single DNA molecules, Nature 443 (2006) 875-878.

[91] Y.T. Kim, S. Tabor, J.E. Churchich and C.C. Richardson Interactions of gene 2.5 protein and DNA polymerase of bacteriophage T7, J Biol Chem 267 (1992) 15032-15040.

[92] X. Shi, Y. Jung, L.J. Lin, C. Liu, C. Wu, I.K. Cann and T. Ha Quantitative fluorescence labeling of aldehyde-tagged proteins for single-molecule imaging, Nat Methods 9 (2012) 499-503.

[93] K. Lang, L. Davis, J. Torres-Kolbus, C. Chou, A. Deiters and J.W. Chin Genetically encoded norbornene directs site-specific cellular protein labelling via a rapid bioorthogonal reaction, Nat Chem 4 (2012) 298-304.

[94] C. Albayrak and J.R. Swartz Cell-free co-production of an orthogonal transfer RNA activates efficient site-specific non-natural amino acid incorporation, Nucleic Acids Res 41 (2013) 5949-5963.

[95] R. Heim, A.B. Cubitt and R.Y. Tsien Improved green fluorescence, Nature 373 (1995) 663-664.

[96] N.C. Shaner, P.A. Steinbach and R.Y. Tsien A guide to choosing fluorescent proteins, Nat Methods 2 (2005) 905-909.

[97] R. Iino, I. Koyama and A. Kusumi Single molecule imaging of green fluorescent proteins in living cells: E-cadherin forms oligomers on the free cell surface, Biophys J 80 (2001) 2667-2677.

[98] H. Murakoshi, R. Iino, T. Kobayashi, T. Fujiwara, C. Ohshima, A. Yoshimura and A. Kusumi Single-molecule imaging analysis of Ras activation in living cells, Proc Natl Acad Sci U S A 101 (2004) 7317-7322.

[99] G.V. Los, L.P. Encell, M.G. McDougall, D.D. Hartzell, N. Karassina, C. Zimprich, M.G. Wood, R. Learish, R.F. Ohana, M. Urh, D. Simpson, J. Mendez, K. Zimmerman, P. Otto, G. Vidugiris, J. Zhu, A. Darzins, D.H. Klaubert, R.F. Bulleit and K.V. Wood HaloTag: a novel protein labeling technology for cell imaging and protein analysis, ACS Chem Biol 3 (2008) 373-382.

[100] Y. Zhang, M.K. So, A.M. Loening, H. Yao, S.S. Gambhir and J. Rao HaloTag protein-mediated site-specific conjugation of bioluminescent proteins to quantum dots, Angew Chem Int Ed Engl 45 (2006) 4936-4940.

[101] A. Keppler, M. Kindermann, S. Gendreizig, H. Pick, H. Vogel and K. Johnsson Labeling of fusion proteins of O6-alkylguanine-DNA alkyltransferase with small molecules in vivo and in vitro, Methods 32 (2004) 437-444.

[102] G. Rigaut, A. Shevchenko, B. Rutz, M. Wilm, M. Mann and B. Seraphin A generic protein purification method for protein complex characterization and proteome exploration, Nat Biotechnol 17 (1999) 1030-1032.

[103] K. Terpe Overview of tag protein fusions: from molecular and biochemical fundamentals to commercial systems, Appl Microbiol Biotechnol 60 (2003) 523-533.

[104] S.R. Adams, R.E. Campbell, L.A. Gross, B.R. Martin, G.K. Walkup, Y. Yao, J. Llopis and R.Y. Tsien New biarsenical ligands and tetracysteine motifs for protein labeling in vitro and in vivo: synthesis and biological applications, J Am Chem Soc 124 (2002) 6063-6076.

[105] M.A. Whitt and C.E. Mire Utilization of fluorescently-labeled tetracysteine-tagged proteins to study virus entry by live cell microscopy, Methods 55 (2011) 127-136.

[106] A.C. Hearps, M.J. Pryor, H.V. Kuusisto, S.M. Rawlinson, S.C. Piller and D.A. Jans The biarsenical dye Lumio exhibits a reduced ability to specifically detect tetracysteine-containi ng proteins within live cells, J Fluoresc 17 (2007) 593-597.

[107] K. Stroffekova, C. Proenza and K.G. Beam The protein-labeling reagent FLASH-EDT2 binds not only to CCXXCC motifs but also non-specifically to endogenous cysteine-rich proteins, Pflugers Arch 442 (2001) 859-866.

[108] J. Yin, A.J. Lin, D.E. Golan and C.T. Walsh Site-specific protein labeling by Sfp phosphopantetheinyl transferase, Nat Protoc 1 (2006) 280-285.

[109] J. Yin, P.D. Straight, S.M. McLoughlin, Z. Zhou, A.J. Lin, D.E. Golan, N.L. Kelleher, R. Kolter and C.T. Walsh Genetically encoded short peptide tag for versatile protein labeling by Sfp phosphopantetheinyl transferase, Proc Natl Acad Sci U S A 102 (2005) 15815-15820.

[110] G. Lee, J. Yoo, B.J. Leslie and T. Ha Single-molecule analysis reveals three phases of DNA degradation by an exonuclease, Nat Chem Biol 7 (2011) 367-374.

[111] B. Treutlein, A. Muschielok, J. Andrecka, A. Jawhari, C. Buchen, D. Kostrewa, F. Hog, P. Cramer and J. Michaelis Dynamic architecture of a minimal RNA polymerase II open promoter complex, Mol Cell 46 (2012) 136-146.

[112] S. Waichman, C. You, O. Beutel, M. Bhagawati and J. Piehler Maleimide photolithography for single-molecule protein-protein interaction analysis in micropatterns, Anal Chem 83 (2011) 501-508.

[113] L. Wang, A. Pulk, M.R. Wasserman, M.B. Feldman, R.B. Altman, J.H. Cate and S.C. Blanchard Allosteric control of the ribosome by small-molecule antibiotics, Nat Struct Mol Biol 19 (2012) 957-963.

[114] I.S. Carrico, B.L. Carlson and C.R. Bertozzi Introducing genetically encoded aldehydes into proteins, Nat Chem Biol 3 (2007) 321-322.

[115] P. Wu, W. Shui, B.L. Carlson, N. Hu, D. Rabuka, J. Lee and C.R. Bertozzi Site-specific chemical modification of recombinant proteins produced in mammalian cells by using the genetically encoded aldehyde tag, Proc Natl Acad Sci U S A 106 (2009) 3000-3005.

[116] A. Dirksen and P.E. Dawson Rapid oxime and hydrazone ligations with aromatic aldehydes for biomolecular labeling, Bioconjug Chem 19 (2008) 2543-2548.

[117] S. Wolter, M. Schuttpelz, M. Tscherepanow, V.D.L. S, M. Heilemann and M. Sauer Real-time computation of subdiffraction-resolution fluorescence images, J Microsc 237 (2010) 12-22.

[118] R. Henriques, M. Lelek, E.F. Fornasiero, F. Valtorta, C. Zimmer and M.M. Mhlanga QuickPALM: 3D real-time photoactivation nanoscopy image processing in ImageJ, Nat Methods 7 (2010) 339-340.

[119] P.N. Hedde, J. Fuchs, F. Oswald, J. Wiedenmann and G.U. Nienhaus Online image analysis software for photoactivation localization microscopy, Nat Methods 6 (2009) 689-690.

[120] R. Parthasarathy Rapid, accurate particle tracking by calculation of radial symmetry centers, Nat Methods 9 (2012) 724-726.

[121] C.S. Smith, N. Joseph, B. Rieger and K.A. Lidke Fast, single-molecule localization that achieves theoretically minimum uncertainty, Nat Methods 7 (2010) 373-375.

[122] A. Kechkar, D. Nair, M. Heilemann, D. Choquet and J.B. Sibarita Real-time analysis and visualization for single-molecule based super-resolution microscopy, PLoS One 8 (2013) e62918.

[123] H. Yardimci, A.B. Loveland, A.M. van Oijen and J.C. Walter Single-molecule analysis of DNA replication in Xenopus egg extracts, Methods 57 (2012) 179-186.